



ELSEVIER

Available online at www.sciencedirect.com

jmr&t
Journal of Materials Research and Technology

journal homepage: www.elsevier.com/locate/jmrt



Review Article

Application of finite element analysis for optimizing selection and design of Ti-based biometallic alloys for fractures and tissues rehabilitation: a review



Kenneth Kanayo Alaneme ^{a,b,*}, Sodiq Abiodun Kareem ^a,
Blessing Ngozi Ozah ^a, Hassan A. Alshahrani ^c,
Oluwadamilola Abigael Ajibuw ^d

^a Materials Design and Structural Integrity Research Group, Department of Metallurgical and Materials Engineering, Federal University of Technology Akure, P.M.B. 704, Ondo, Nigeria

^b Centre for Nanoengineering and Tribocorrosion, School of Mining, Metallurgy and Chemical Engineering, Faculty of Engineering & the Built Environment, University of Johannesburg, South Africa

^c Department of Mechanical Engineering, College of Engineering, Najran University, King Abdulaziz Road, P.O Box 1988, Najran 61441, Saudi Arabia

^d Institute for Materials Science, Faculty of Engineering, University of Kiel, Kaiserstrasse 2, 24143 Kiel, Germany

ARTICLE INFO

Article history:

Received 28 March 2022

Accepted 1 May 2022

Available online 11 May 2022

Keywords:

Computational materials science

Biometallic materials

Ti and Ti-Based alloys

Finite element analysis

Biomechanical properties

Biodegradation

ABSTRACT

This review attempts to provide a state-of-the art literature evaluation of the application of finite element analysis to the selection and design of Ti and Ti-based biometallic alloys for biostructural rehabilitation, a background required for understanding the limits of practical implementation of the outcomes of computational analysis for biomaterials design. Biometallic materials based on titanium and titanium alloys are arguably the most pragmatic option for implant and scaffold design intended for bone, tissue, and vascular repairs, and other musculoskeletal disorders. This is owing to their high biocompatibility, low toxicity, high strength-to-weight ratio, and general mechanical properties that are similar to those of human tissues. Their selection, design and practical deployment for biostructural use is conditionally dependent on the outcomes from extensive biomechanical assessment before clearance for clinical property evaluation is recommended. These assessments, which are experimental in nature, require a lot of commitment both in terms of materials, cost, man-hours, and state-of-the-art facilities. A rapid and less resource-demanding approach to assessing the bio-mechanical suitability of biometallic materials as tissue replacements in the body could be of great help, and the use of finite element analysis based computational modelling and simulation techniques appears to be the way forward. This review analyses the basis, procedures, and outcomes from such computational studies on Ti based biometallic systems targeted for fractures and tissue rehabilitation. It also assesses the strengths, challenges and future scope for the utilization

* Corresponding author.

E-mail address: kalanemek@yahoo.co.uk (K.K. Alaneme).

<https://doi.org/10.1016/j.jmrt.2022.05.001>

2238-7854/© 2022 The Authors. Published by Elsevier B.V. This is an open access article under the CC BY-NC-ND license (<http://creativecommons.org/licenses/by-nc-nd/4.0/>).

of finite element analysis outcomes for selection and design of Ti based biostructural materials.

© 2022 The Authors. Published by Elsevier B.V. This is an open access article under the CC BY-NC-ND license (<http://creativecommons.org/licenses/by-nc-nd/4.0/>).

1. Introduction

With an aging population, rising standards of living in developing countries, and an increased ability to treat previously untreatable medical diseases, the field of biomaterials has witnessed considerable growth [1]. Biomaterials are natural or synthetic materials used to create implants or structures that enhance, maintain, or restore damaged tissue and other biological functions [2]. They are essential in modern medicine to restore biological functions and aid in the healing of patients [3]. Biomaterials are used in a variety of applications in the human body, including prosthetic heart valves, stents in blood vessels, shoulder, knee, hip, elbow, and ear replacement implants, and orodental constructions [4,5]. The number of biomaterials utilized for shoulder, hip, and knee-joint replacement implants is exceptionally high among these applications [6,7]. These aforementioned joints constitute rigid tissues that are prone to damage due to their intricate structure and demanding working conditions [8,9]. As a result, demand for load-bearing implants in hard tissue replacement is expected to grow. This spike in demand requires an increase in biomaterials development activity.

The choice of a material for a specific application in engineering design is determined by tailoring the material's characteristics to the application's needs [10]. When it comes to biomaterials, however, concepts such as biocompatibility, stress shielding, bioactivity, and osteoinduction, in addition to their mechanical, chemical, and physical properties, are considered the most important criteria for their selection in medical implant design [11,12]. These implants should satisfy a number of conditions, such as excellent corrosion resistance in the body environment, a favorable mix of good strength and low elastic modulus, excellent wear and fatigue resistance, good ductility, and be cytotoxicity-free [13,14]. These implants must be able to withstand cyclic biomechanical stresses during their life span as well as possess a tendency to re-establish the human bone's functionality [15,16]. Metals, polymers, ceramics, glasses, and even tissue and living cells can all be used in the production of biomaterials [17,18]. However, metallic biomaterials are widely employed to replace hard tissue and in other biostructural load-bearing applications [19,20]. While a number of metals (such as stainless steel, chromium-cobalt, magnesium alloys, nickel-titanium, and titanium alloys) have been utilized as biomaterials, titanium alloys are rapidly emerging as the material of choice for the great majority of applications [21].

Titanium (Ti) is widely used in a wide range of applications since its properties may be altered by modifying the alloy elements composition [22]. Titanium alloys have often been used as dental as well as orthopedic implants owing to their

high specific strength, exceptional corrosion resistance, as well as excellent biocompatibility properties [23,24].

The combination of low elastic modulus and excellent mechanical strength has been sought in contemporary Ti-based alloys. This makes it possible for the Ti-based alloys to potentially offer superior long-term biomechanical stress support, avoiding stress shielding and revision operations [25,26]. The stress shielding phenomenon, which is caused by a mismatch in elastic modulus between the implants and the surrounding bone components, has been reported to be a major drawback of metallic implants, as it results in osteopenia and bone resorption [27,28].

Biomechanical and biological factors play a significant influence in the prediction of successful implantation [29]. Consequently, there is growing interest in exploring computational techniques for rapid assessment of these factors and their impact on the behaviour of biomaterials [30,31]. Since the finite element method (FEM) is applied to solve engineering issues in many domains of science and industry today, it has become a powerful approach in predicting the biomechanical behaviour of bone-implant as well as the detection of stress/strain hotspots [32,33]. This review paper focuses primarily on titanium-based alloys. It discusses the use of modeling and simulation for selection, design and predicting the biomechanical compatibility of a variety of Ti-based alloys for fractures and tissue rehabilitation, emphasizing the overall advantages of titanium-based alloys and the benefits of FEA method. Specifically, the use of FEA method in: rehabilitating femoral fracture, mandible fracture; porous Ti scaffolds and implants designs; and miscellaneous rehabilitations (such as hip prosthesis, orthodontic implants, cervical spondylosis, maxillofacial plates and implantable devices, lumber spine segments, among others) are examined in detail. Furthermore, this review highlights the strengths, limitations and future research directions related with the use of FEA method in optimizing selection, design and predicting the biomechanical behaviour of Ti-based biometallic materials.

2. Prediction of the biomechanical behaviour of Ti-based materials with finite element analysis

In the early stages of mechanical and structural engineering, including orthopedic biomechanics in the 1970s, the Finite-Element-Method (FEM) was frequently used to evaluate stresses in human bones under functional loading [34,35]. After the 1980s, Finite-Element-Analysis (FEA) was increasingly used in implant modeling and development, as well as orthodontics pertaining to deformation under functional applied loads. This approach has received extensive

acceptance in engineering as well as biomedical disciplines and is largely utilized in stress assessments of bone as well as prosthetic structures, dental-implants, and other functional medical devices [3,36]. Also, by employing nano-mechanical testing such as nano-indentation, the FEM has been used to evaluate the biomechanical characteristics of nano-coatings such as hydroxyapatite on titanium implants [37]. Some studies which have reported on the use of FEA for biomechanical analysis of the performance of specific Ti-based alloys are reviewed in this section.

2.1. Femoral fracture

The longest bone in the human body, the femur, carries the weight of the upper body while permitting leg mobility [38]. Femur fractures can be caused by large pressures, accidents, falls from high altitudes, impact loads and musculoskeletal diseases [39,40]. The treatment of a femoral shaft fracture is almost always with surgery. Femur fractures, including partial fractures, severe impact fractures, and fully dislocated fractures, need the insertion of prosthetic implants [39,40]. Intracapsular femoral neck fractures (FNFs) are one of the most prevalent forms of orthopedic injuries, accounting for more than half of all proximal femoral fractures (PFF) [41]. The ideal form of fixation implants for the rehabilitation of femoral neck fractures (FNFs) is still under debate. The use of FEA in implant assessment and design enhancement might boost biomechanical rationale for implant selections in cases such as femoral neck fractures (FNFs). Zeng et al. [42] conducted a study to analyze the biomechanical impact of medial buttress plate (MBP) augmentation as well as the biomechanical performance of numerous implantable devices for Pauwels type III femoral neck fractures under physiological loading scenarios using FEA. The finite element approach was used to quantitatively examine many fixation styles for FNFs. Five model groups were created using various FNFs fixation implants, including proximal femoral nail anti-rotation (PFNA), dynamic hip screws (DHS), cannulated screws (CSs), DHS plus MBP augmentation (DHS + MBP), and CSs plus MBP (CSs + MBP). Four Finite Element models were developed for each group to measure bone strain and device stress during walking as well as stair ascending scenarios, which replicated hip contact force employing static as well as dynamic loadings, respectively. The cortical and the trabecular bones of the femur were both assumed to be linear elastic material models. The titanium alloy was considered to be a linear plastic material with a yield strength, elastic modulus, as well as poison ratio of 0.885 GPa, 104 GPa, and 0.33, respectively. The contact interactions were described using a friction contact, with the friction coefficient set at 0.46 between the fracture sites, 0.23 between implant components, as well as 0.30 between bone and implants. The results show that there were no significant changes in peak strain inside implanted bone as well as the maximum stress magnitude of the device between CSs and DHS. The implanted femur with PFNA was observed to be in a lower condition of bone strain and implant stress (Fig. 1). The maximal equivalent stress on each implant was somewhat higher when it was loaded by stair ascending than when it was loaded by walking. There was an extremely high level of stress on the CSs during dynamic conditions, which was close

to the device's yield strength. Although the buttress plate did not reduce peak bone strain, it did reduce stress concentration on the device, particularly for CSs subjected to dynamic loadings. This suggests that buttress plates can serve as an extra load route for the transmission of force between fracture pieces. In spite of this, the MBP failed to reduce much of the strain concentration between the compressed bone pieces. It also caused a concentration of strain in the localized region of bone that is in contact with MBP and its screws. When it comes to fracture fixation in fractured neck fractures, there is still no clinical data to support one approach over another. However, it was established that, when compared to alternative fixation techniques, the PFNA provided biomechanical benefits by lowering the likelihood of implant failure as well as bone yielding. The MBP augmentation provides an extra load route to bridge fracture fragments, lowering the probability of DHS and CS failure, particularly in dynamic loading circumstances. Although further research is required for patients with other forms of FNFs, the obtained results in this study will be of immense benefit for optimizing device design for complex physiological loadings and clinical decision-making in FNFs surgical therapy.

In a similar study, Cui et al. [43] used FEM to investigate the bio-mechanical variation observed between three implant designs for the management of diverse femoral neck disorders together with Pauwels type II as well as type III fractures. The proximal femoral nail anti-rotation (PFNA) fixation, inverted-triangle-screw (ITS) fixation, as well as dynamic hip screw (DHS) fixation, are the internal fixation designs studied. The internal fixation device in this investigation was made of the medical grade titanium-based alloy, Ti-6Al-7Nb, which has an elastic modulus of 110 GPa as well as a poison ratio of 0.33. A patient weighing 60 kg and standing on one foot was subjected to a 600 N axial force applied to the contact area between the femoral head and acetabulum in the axial direction. The hip joint reaction force was set at 2872 N, and the abductor loading was set at 1237 N for a patient weighing 60 kg in the single-foot landing state. The coefficient of friction was fixed at 0.2, and the fracture sections were in touch with each other. The findings show that when the Pauwels angle rises, so does the femoral head displacement. The reason for this is that, when there is a rise in the angle of the fracture, the angle between the screw and the broken part gets closer to 90°. As a consequence, the internal fixation device carries more stress and is more prone to distortion, resulting in greater femoral head displacement. It was established that people with osteoporosis have a greater frequency of femoral varus as well as femoral neck shortening than individuals with healthy bones. The observed peak stress of the internal fixation device in the osteoporosis patient is higher than in the healthy bone patient, indicating that the device is more susceptible to fracture in the osteoporosis patient. The reason for this is that, in the osteoporosis model (OM), the elastic moduli of cortical as well as trabecular bones are lowered, resulting in a reduction in peak and average stress observed in the femur section. The internal fixation device bears a greater load as it is the portion with the highest elastic modulus in the OM, resulting in increased stress. In terms of capacity to withstand femoral neck shortening, PFNA fixation is found to be the strongest among ITS, PFNA, and DHS fixations, whereas DHS fixation is

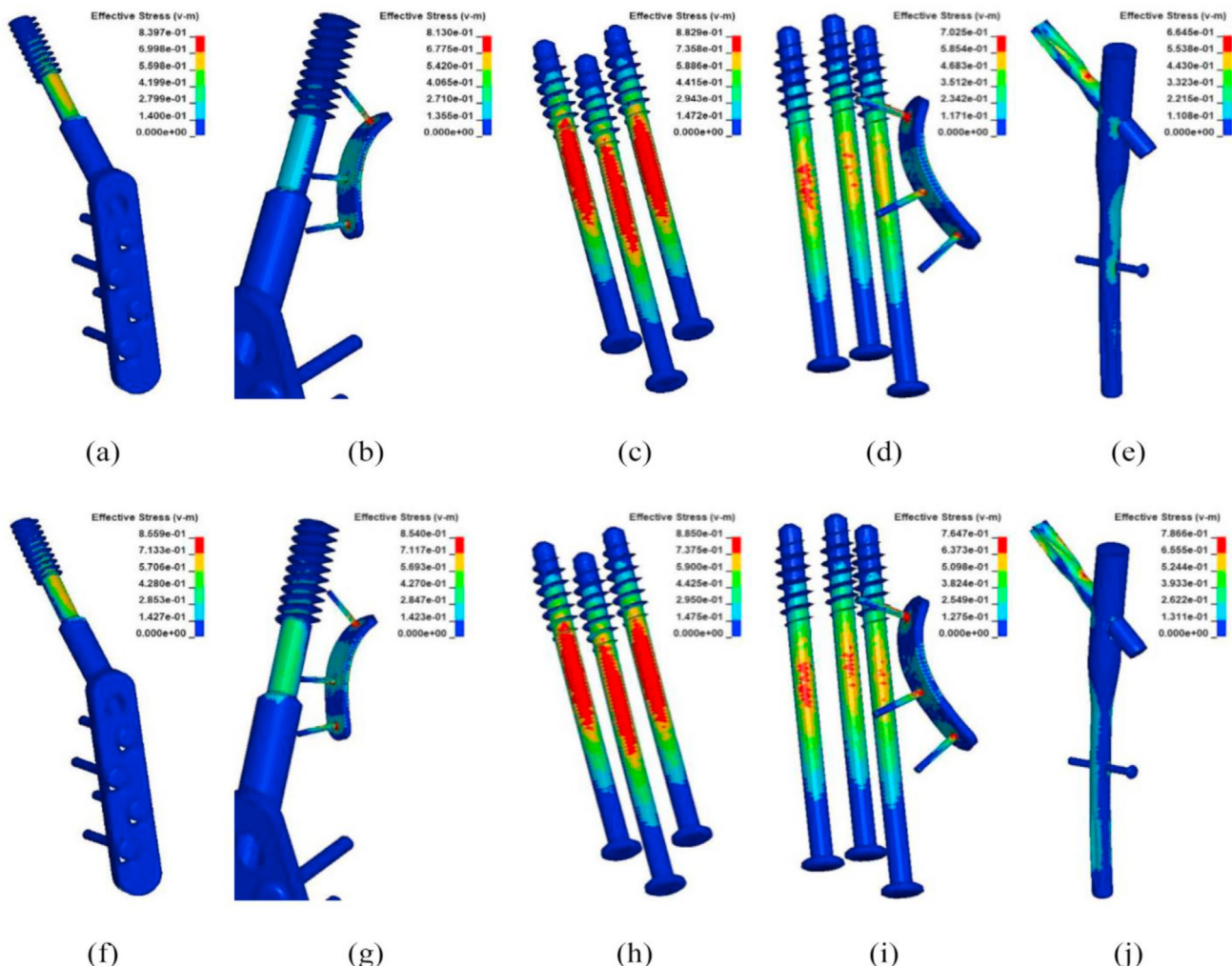


Fig. 1 – Von Mises stress distribution (10^3 MPa) on the implants: (a)–(e) showed the results under walking with dynamic hip contact force for DHS, DHS + MBP, CSs, CSs + MBP and PFNA, respectively, and (f)–(j) showed the results under stair climbing with dynamic hip contact force for corresponding fixation styles. The maximum stress in each subgraph was indicated by the maximum value in each legend for comparison. (Zeng et al. [42] culled with permission from Elsevier).

shown to be the poorest. The ITS fixation is more suited for the treatment of individuals with healthy bones who have a Pauwels II femur neck fracture. The PFNA fixation, on the other hand, provides higher biomechanical benefits and is more capable of preventing femoral neck shortening which is consistent with the findings reported by Zeng et al. [42]. As a result, it is appropriate for the treatment of osteoporotic femoral neck fracture patients. To verify the finite element model, the authors conducted mechanical tests on a cadaver specimen. The FEA findings were compared to the experimental data. The stress at each position in the finite element model was found to be about the same as the measured value for the cadaver specimen, proving the validity of the finite element model utilized in this investigation. However, the FEM model did not account for the impact of muscles and ligaments, and it did not distinguish between varus and femoral neck shortening. Also, fracture rehabilitation is a complicated process influenced by several physiological and biomechanical elements, and the mechanical analysis in this

research addressed just a portion of it. As a result, it is critical to evaluate the role of biological variables on the internal fixation effect of femoral neck fractures in future studies.

The most common procedure for femoral shaft fractures' rehabilitation is intramedullary nailing. The marrow canal of the femur is pierced with a specifically constructed nail. This nail can be implanted through a tiny incision at the hip or knee of the canal. This nail is mostly made of titanium, which is an expensive material. As a result, shattered bone surgery is very pricey. Shahjad and Ganorkar [44] carried out an investigation in order to offer the best substitute material at a reasonable cost. Titanium alloy (Ti–6Al–4V), cobalt chrome, and 316L stainless steel were used as the materials. A 3D scanner was used to model the femur bone, and the intramedullary nailing was modeled using SolidWorks CAD software. ANSYS software was used to do the analysis. The results revealed that the head of the femur experiences the most deformation, whereas the lower end experiences the least. The maximum equivalent stress is 67733 Pa, whereas the

lowest principal stress is 99.98 Pa. The femur's central part generates the greatest maximum principal stress. A comparable Von-Misses stress of 67733 Pa was found. The stress distribution and deformation of the femur with implants of various material characteristics during normal position at varying weights were then determined. The models were only subjected to static loads. This static loading condition and material comparison investigation revealed that titanium implant mechanical characteristics are superior to those of other materials assessed.

2.2. Mandible fractures

Sagittal split osteotomy (also known as bi-lateral sagittal split osteotomy, or BSSO) is a popular surgical treatment used to address dento-facial abnormalities involving the mandible. To achieve stability following BSSO, bi-cortical bone fixation screws or mini-plates combined with mono-cortical bone fixation screws were often employed. Demircan et al. [45] investigated stress distribution levels at the temporomandibular joint (TMJ) as well as mandibular bone segment displacement levels. The mandible was designed as a 3-D virtual mesh model. The finite-element model was then used to simulate BSSO with a 9 mm advancement. Fixation in between each mandibular segment was also virtually implemented utilizing seven distinct fixation material combinations, as stated: mini-plate (M), mini-plate plus Ti-based bi-cortical bone fixation screw (H), mini-plate plus a resorbable bi-cortical bone fixation screw (HR), three L-shaped titanium bi-cortical bone fixation screws (L), three L-shaped resorbable bi-cortical bone fixation screws (LR), three inverted L-shaped Ti-based bi-cortical bone fixation screws (IL) and three inverted L-shaped resorbable bi-cortical bone fixation screws (ILR). The results of the findings show that, at 9-mm advancement, M fixation produced the highest stress values at the anterior region of the TMJ, whereas LR fixation produced the highest stress values at the posterior TMJ. The anterior TMJ had the lowest stress levels at L fixation while the posterior TMJ had the highest stress values at M fixation. The IL approach produced the least amount of displacement, followed by L, H, HR, M, ILR, and LR, in that order. Based on the findings obtained, bi-cortical screw fixation was linked with a significant increment in stress distribution on the condyle. With regards to overall stress value, LR and ILR contribute the most. As a result, physicians need to be informed that changed TMJ loading might result in condylar resorption as well as late relapse following mandibular advancement cases.

A unique 3-dimensional titanium mesh scaffold containing bone-grafting materials has just been developed for the reconstruction of a major mandibular defect. However, the process of designing as well as optimizing 3-D mandible scaffolds is yet unknown. Gao et al. [46] investigated ways to make 3-dimensional scaffolds for mandibular abnormalities more effective. The biomechanical behavior and mechano-biological characteristics of scaffolds were investigated in this work. There were twelve groups, each with three strut sizes (0.2 mm, 0.5 mm, and 0.8 mm) as well as four different geometries (regular dodecahedron (Rd), cuboctahedron (Co), regular hexahedron (Rh), and diamond (Di)). In this study, Finite-Element-Analysis (FEA) in combination with the bone

Mechanostat-theory were used to choose the best unit cell from a total of twelve scaffolds. A modified version of the original implant specifically for the mandibular anomalies was produced utilizing the best unit cell, and then the final implant was fine-tuned to stimulate osteogenesis while avoiding premature failure scenarios under bilateral chewing bites (200N) and maximum force (worst case) biting scenarios (800N). The results revealed a clear correlation between geometrical configuration and load transmission capabilities. The strut size as well as its architecture were observed to have a significant impact on mechanical failure. The observed maximum von Mises stresses on scaffolds steadily reduced as the strut diameter increased in all groups. To avoid scaffold failure in diverse conditions, the maximum stress in each configuration must be less than the yield strength. Unfortunately, with the exception of the regular dodecahedrons having 0.8 mm strut diameter model, the other groups' maximum stress values surpassed the yield strength, making them the most prone to failure. Regular dodecahedrons having 0.8 mm strut diameters were discovered to transfer the appropriate stress to bone tissue without failing mechanically. Furthermore, the best implant was created with the normal dodecahedron unit cells, and the scaffold's strut diameters were gradually modified depending on the biomechanical analysis. According to computational analyses, the ideal implant can provide a favorable mechanical condition for bone regeneration, leading to long-term stability as well as occlusal rehabilitation with a dental implant. The findings of this work will be of immense benefit when developing and designing 3-dimensional mesh scaffolds for better functionality as well as aesthetic mandibular rehabilitation.

Using 3-D Finite-Element-Analysis, Yamaguchi et al. [47] investigated how different materials and fixing procedures affect the maximum principal stress as well as displacement in reconstruction plates. The mandibular segment as well as the teeth were created using computer-aided-design (CAD). CAD software was used to design the Champy as well as the AO/ASIF plates and also the fixation screws. Image-based CAE software was used to perform the 3-dimensional FE-Analysis. The Champy as well as AO/ASIF plates fabricated from pure titanium grade-2 (cp-Ti) as well as a titanium-15molybdenum alloy were compared in terms of bio-mechanical integrity, maximum principal stress, and displacement distributions. From the findings, the maximum and minimum values for the maximum principal stresses in the pure Ti-based Champy plate, lower AO/ASIF plate, and upper AO/ASIF plate for plates that were fixed on the model of a fractured mandible within the left angle were presented to be 19.5 and 20.3 percent, 21.4 percent and 4.6 percent, and 15.2 percent and 25.3 percent lower, respectively, compared to those in Ti-15Mo plates. The highest and lowest displacement values in the pure Ti-constructed-Champy plate, the upper AO/ASIF plate, as well as the lower AO/ASIF plate, were also observed to be higher than those that were obtained for the Ti-15Mo-constructed plates in the same model. The incorporation of molybdenum into titanium is thought to lower the young modulus of the resulting alloy [48,49], giving it material characteristics comparable to human mandibular bone [50]. This makes Ti-15Mo preferable than Ti-6Al-4V in terms of characteristics, and it appears to decrease the strain concentration that triggers

bone resorption [51,52]. Hence, Ti–15Mo plates depict better strength and load-bearing capability and could therefore enable a shorter treatment period with greater longevity in clinical service.

Total joint replacement (TJR) is a complex procedure, and complications, which include hardware failure, cleft, infection, or facial immobility, might occur. As a result, it is critical to investigate the stresses that occur during jaw movement. Soni and Sharma, [53] investigated the stress concentration for a novel temporo-mandibular joint (TMJ) prosthesis through finite element analysis. The method used was a 3-dimensional static structural FE technique. Solid Works 2012 was employed to design the TMJ prosthetic pieces – fossa and condyle, while 3D SLICER 4.10.2 was utilized to develop a musculoskeletal model. ANSYS software was used to create a three-dimensional mesh model of a prosthesis set on a jaw model. Mandible, Surface boundaries for the mandible, fossa, condyle, and all associated muscles were determined. The masticatory muscles were represented by the magnitudes of their forces retrieved from the literature. In this investigation, the biting force range was 200–1000 N. The metal-plastic prosthesis assembly is divided into two parts: the upper jaw fixation, known as a fossa implant, which is made of Ultra-High Molecular Weight Polyethylene (UHMWPE), and the lower jaw fixation, known as the mandibular implant with a condylar head, made of a grade 5 Titanium (Ti) alloy with an elastic modulus and Poisson ratio of 110 GPa and 0.3, respectively. The mandibular implant is custom-designed and 3-D manufactured to fit the exact form, curve, and location of the mandible's ramus. The obtained results revealed that the response forces in screw-affixed locations following mastication were 650 N, 375 N, and 110 N, respectively. The resultant magnitude of the reaction forces observed in the condylar head peripheral was 1034 N. During mastication, total muscle forces produced a stress of 5.76×10^6 N/m² at the condylar head of the contralateral natural joint for the unilateral joint when loaded to 1000 N. A stress of 3.076×10^6 N/m² for a bilateral joint under identical boundary circumstances. Von Mises stresses for unilateral and bilateral TMJ are described for four distinct loading scenarios, namely normal loading, imbalanced occlusion, bruxism, and clenching. Clenching, as predicted, resulted in substantial stresses around the disc surfaces, and greater stresses were found in the bilateral TMJ in all four loading scenarios. Von Mises stresses relate to tissue strains rather than contact pressures; hence, stresses are larger in the case of bilateral TMJ. According to the authors, a customized TMJ prosthesis is better in TMJ complete joint replacement because it can give almost the same degree of displacement in opening and shutting of the jaw, and as a consequence, the mandible will be under less tension. This will also allow for less muscle force involvement while moving the lower jaw. The output from the computational analysis was verified by comparing the collected data to those obtained from literature. Experimental validation and clinical trials, on the other hand, are required to assess the feasibility of design, appropriateness, and biocompatibility of prostheses. Furthermore, the study did not use real patient data for definitive examinations of human TMJ. The effectiveness of design, as well as computational studies, must be evaluated using real TMJ patient CT data for prosthesis customization.

Mandibular endoprostheses have been extensively studied for alloplastic reconstruction. People with segmental mandibular abnormalities, on the other hand, may find it difficult to loosen their teeth. Another technique entails inserting a tray containing bones over the defect as well as connecting wings on each side with the aid of screws, which has lately become prominent in therapeutic settings as a design solution for patient-specific dental implants for segmental mandibular anomalies. Although Selective Laser Melting (SLM) fabricated PSCIs (patient-specific customised implants) enjoy a favourable reputation in the clinical sector, the uneven distribution of heat caused by the implant's intrinsic domain-by-domain localised development causes significant tensile residual stress. Hence, under cyclic loading, residual tensile stress will not only increase fatigue fracture propagation but also induce macro-scale implant deformation, lowering implant placement accuracy [54]. This kind of deformation is most noticeable in bar-like materials owing to the comparatively substantial stress build-up across the length when compared to that directed along the thickness and breadth [55]. A stress-relieving heat treatment is frequently given before the printed pieces are removed from the base plate to minimize unfavorable part deformation. For titanium alloys, heat treatment is often used after the selective laser melting process to relieve residual stress and create isotropic mechanical characteristics by eliminating epitaxial columnar grains [56]. However, a subsequent heat treatment will not be able to completely restore the plastic distortion that occurs at the ends of the bar-shaped components, which has an effect on the overall implant structure [54]. As a result, the requirement to minimize implant deformation and optimize biomedical characteristics is critical. Palka et al. [57] recently investigated the biomechanical feasibility of employing shorter SLM plates to treat a small-sized mandible fracture. A finite element model was created to repair a human mandible that has been fractured, as well as examine how varying configurations of modular fixation plates (star-shaped plate and rectangular plate) react when subjected to bite loading forces of 200 N, 150 N, and 100 N, as well as analyzing the stress distribution using ABAQUS software. The mandible's numerical model was simplified such that its structure resembled the edentulous shaft. The primary chewing muscles, which include the masseter, temporal, medial pterygoid, and lateral pterygoid, have been eliminated. The volumetric tetrahedral type elements were employed in the 3-dimensional model's discretization, with the number of finite elements for the mandible set at 73284, and the average size of the element set at 0.3 mm. They created new modular star-shaped plates (10 mm in diameter) and matching dog-bone-shaped plates (19 mm in length) to substitute for a long and flat bar-shaped plate about 25 mm in length. In the investigation, a linear-elastic isotropic material model was applied. For all configurations, the same boundary conditions were used. The finite element analysis revealed that the treated bone had high construction stability, which benefited bone segment stability, anatomic gap reduction, as well as physiological bone function restoration. Hence a combination of short Ti-based plates fabricated by additive manufacturing offers several benefits for total mandible restoration, including reduced intrinsic implant deformation and its

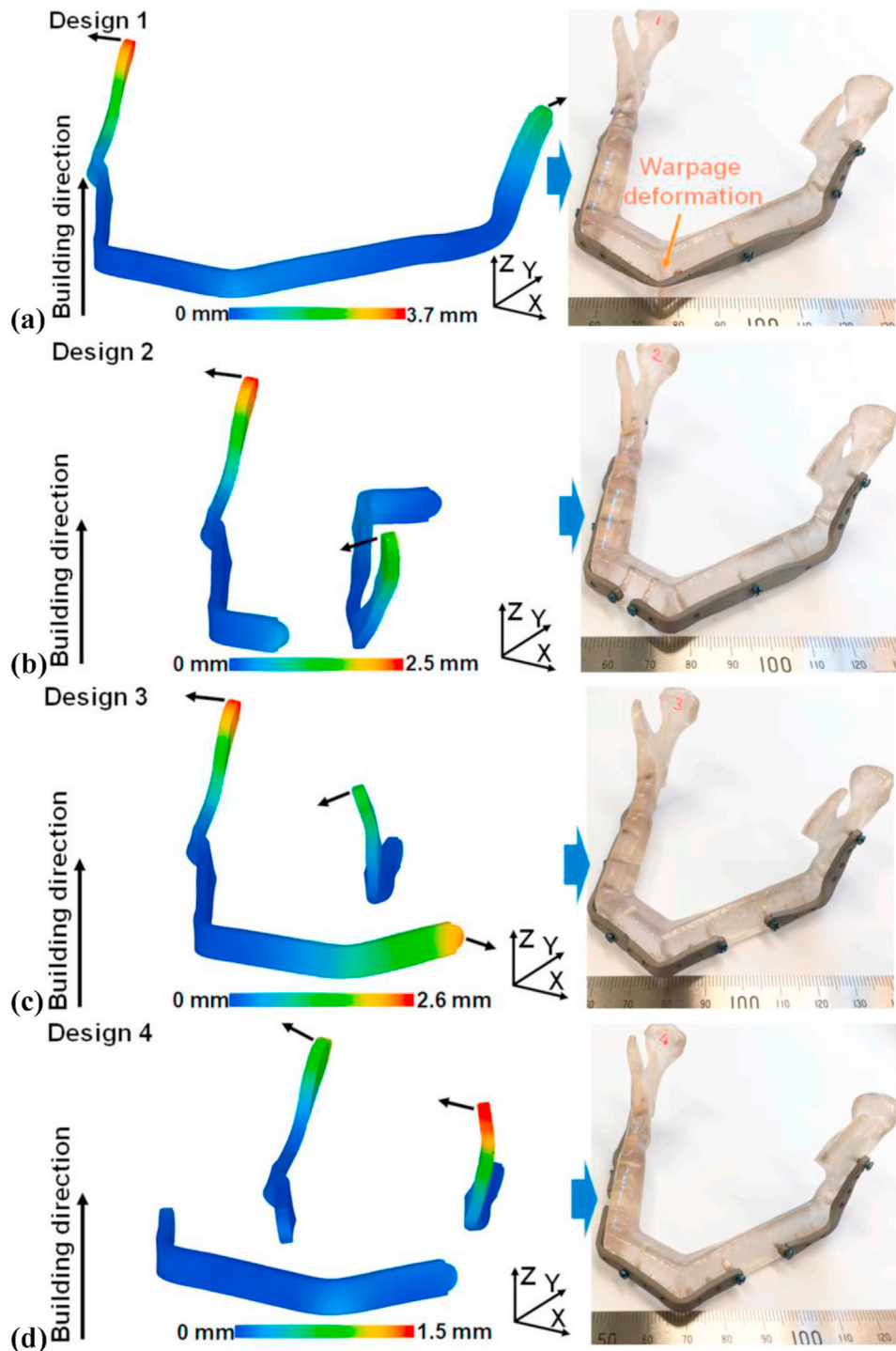


Fig. 2 – Implant deformation prediction during SLM and in vitro experimental validation: (a) Design 1, (b) Design 2, (c) Design 3, and (d) Design 4. (Black arrows highlight the displacement direction. Screw holes on the MRPs were drilled and tapped after SLM by a CNC machine to provide processing quality, so there were no screw holes on the MRPs during the implant deformation prediction). (Shi et al. [58] culled with permission from Elsevier).

consequence on clinical procedures, as well as increased surgical flexibility.

However, it is uncertain if shorter titanium implants fabricated by additive manufacturing can be utilized to correct massive bone defects. Shi et al. [58] conducted research to

determine the bio-mechanical potential of using a mix of short mandible reconstruction plates (MRPs) to substitute a standard single long plate for total mandible rehabilitation. The ANSYS Workbench was used to conduct FEA simulations of human masticatory processes. In all, four model assemblies

were meshed, yielding 165790–177494 elements as well as 36990–39134 nodes. Because of its clinical usefulness and biocompatibility, Ti–6Al–4V was chosen as the material for the MRPs and screws. To rule out the impact of material metallurgical flaws in the bio-mechanics simulation, the plates and screws were assumed to be devoid of flaws. Thus, the linear-elastic, isotropic, and homogeneous material characteristics were assigned: Young's modulus = 113800 MPa, fatigue strength = 510 MPa, Poisson's ratio = 0.34, and yield strength = 870 MPa. Three distinct combinations of short mandible reconstruction plates (MRPs) were customized while implant deformation was taken into account throughout the additive manufacturing process. The biomechanical performance of the resulting model was compared to that of a single long MRP using finite element analysis (FEA). Implant deformation caused by SLM may be decreased by 30–59 percent on short mandible reconstruction plates, lowering the maximum displacement to 1.5–2.6 mm on Designs 2–4 from 3.7 mm on Design 1 (Fig. 2). The reduced implant deformation may improve implant placement accuracy and, consequently, clinical outcomes. In total mandible reconstruction, the use of a long plate and a small plate in tandem (Design 3) demonstrates better bio-mechanical qualities than a traditional single long plate (Design 1) and provides the most consistent fixation durability among the three designs with short plates (Designs 2–4). Design 3 outperforms conventional Design 1 in terms of plate safety as it was observed that maximum tensile stress on plates (design 3) is minimized by 6.3 percent, system fixation instability (relative total displacement is reduced by 41.4 percent), and bone segment stability (bone segment dislocation is less than 42.1 m) during masticatory activities. As a result, the bio-mechanical potential and fixation durability of employing short MRPs for total mandible repair may be established in a preclinical setting. It is worth noting that plate length should be properly selected in order to acquire accurate biomechanical characteristics. The findings of this

study are likely to provide valuable knowledge for the management of additional large-sized bone lesions with short, customized implants, hence broadening the prospect of additive manufacturing for use in implant applications. Prediction of implant deformation during selective laser melting (SLM) and in-vitro experimental validation. Randomized clinical trials as well as in-vivo studies are recommended to validate the real clinical efficacy as well as utility of employing short SLM-fabricated mandible reconstruction plates for total mandible repair.

2.3. Porous titanium scaffold and implants

The use of a porous scaffold was studied as a viable technique to heal bone defects, albeit its stability as well as biomechanics throughout the healing period was unclear. Peng et al. [59] presented a mandibular titanium implant with multilayer porous structures that are structurally and mechanically equivalent to bone tissue. The porous implant's design as well as mechanical behavior evaluation were established based on CT data as well as a rebuilt 3-D model, using several software packages as shown in Fig. 3.

The designs of the porous implant as well as the fixed structures were enhanced by the use of topology. Using FEA integrated with bone mechanostatic theory, the stress as well as osteogenic characteristics of the multilayer porous scaffold with three distinct fixation schemes (Model-I with 4 screws, Model-II with 5 screws, as well as Model-III having 6 screws) for mandibular rehabilitation were studied. The Poisson's ratio was fixed at 0.3. In contrast to Model I, the study found that Model III, as shown in Fig. 4, could successfully minimize the stress-shielding impact, with stresses within the defective mandible, optimized implant, and screws, reducing it by 44.23%, 48.18%, and 57.27%, respectively. Also, the porous implant exhibited a considerable stress transmission influence and retained the same stress distributions as the intact

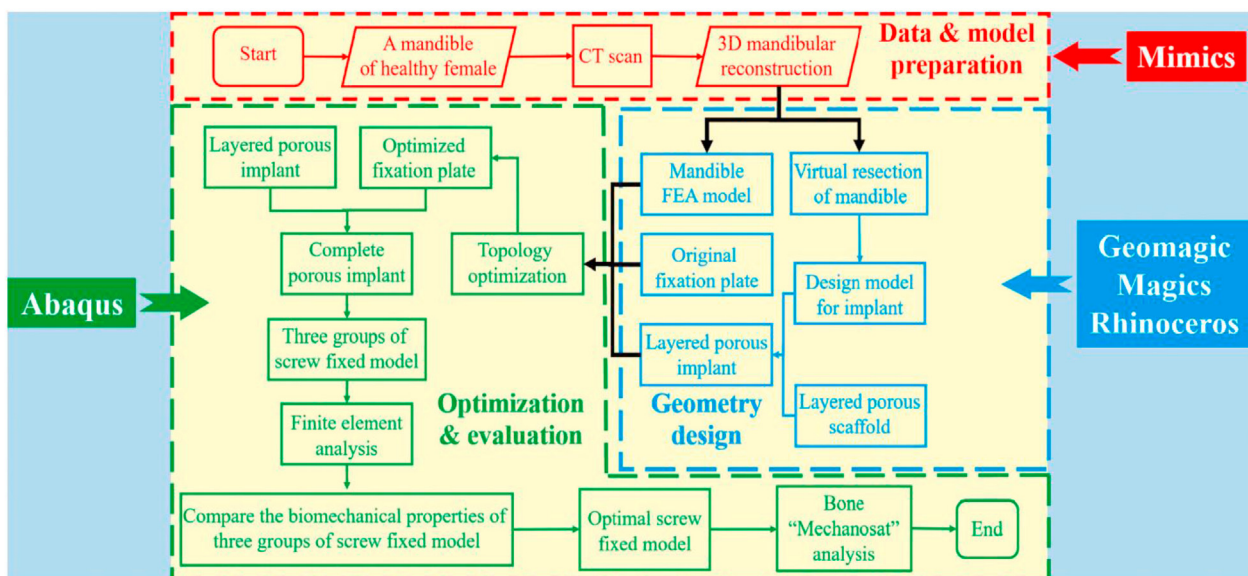


Fig. 3 – Flowchart demonstrating design and analysis of the layered porous implant used (Peng et al. [59], culled with permission from Elsevier).

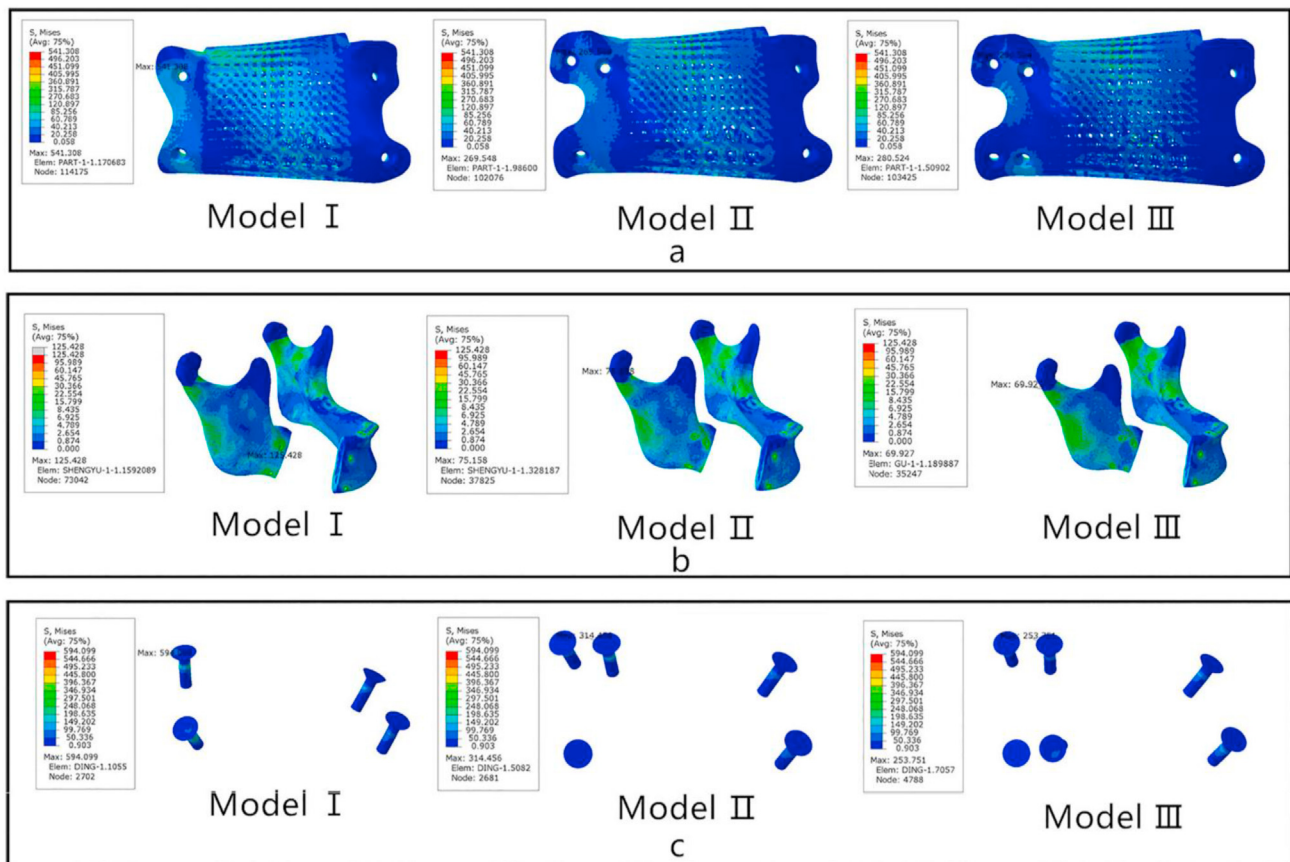


Fig. 4 – The comparison between the stresses on three groups of fixing screws, after the repair. (a) Layered porous implant. (b) Defective mandible. (c) Screws (Peng et al. [59], culled with permission from Elsevier).

mandible. According to the bone "Mechanostat" theory, the porous implant had a strong mechanical stimulating effect on bone tissue growth and repair. The combination of a porous structure and a topological approach appears to be a potential choice for improving the implant's mechanical stability and osteogenesis, and it may offer a novel approach to mandibular rehabilitation.

One of the core reasons for implant failure, infection, as well as loosening, is osteopenia induced by weak tissue engineering and implant integration [60]. Only when the host tissues and the implanted scaffolds are physiologically and mechanically coherent can full integration be accomplished [61,62]. The scaffold's porous structure allows cells to migrate within and proliferate, and also gives room for pre-osteoblastic cell colonies to develop into osteoblast and grow to mineralize the osteogenesis, which leads to osteoconduction [63,64]. Porous Ti as well as its alloys are gaining prominence as the most widely applied material for the fabrication of implant devices specifically for orthopedic applications due to their high corrosion resistance as well as chemical bio-inertness, in addition to their tunable material stiffness achieved through the introduction of porous structure to avoid stress-shielding [65,66]. Soro et al. [67] carried out an investigation into the mechanical characteristics of porous titanium structures with varying porosity degrees using a combination of experimental tests together with FE modeling.

FE based models were used to investigate the bio-mechanical behaviour of a novel sintered porous titanium structure. Finite element simulations using first-order tetrahedral elements (C3D4 elements) were performed using the ABAQUS program. The sintering fabrication approach results in a spheroidal pore structure, which has a massive effect on both the elastic modulus as well as the yield strength of the material. This results in anisotropy within the elastic characteristics, with the degrees of anisotropy (as measured by the ratio of the axial to that of the transverse Young moduli) attaining up to 22 percent for porous specimen having 40 percent porosity. When compared to the spherical pores, it was observed that oblate spheroidal pores produce a better result and have an excellent correlation with experimental data in the Finite-Element simulations. In terms of prediction capability, the Finite-Element findings outperform the semi-analytical Mori-Tanaka model. When the local fields forecast by the Finite-Element models were evaluated, high-stress concentrations as well as localized plastic deformation were also detected within the porous structures' thin walls. The experimental curves' lack of hardening capability actually reinforced the concept that high stress and strain concentration levels will trigger localized premature material degradation. The randomly dispersed pore network formed during the fabrication process is likely to have such thin walls, and the possibility increases with an increase in the degree of porosity.

These findings suggest that regular interior layouts are required to reduce stress concentration levels and give a higher strength-to-density ratio. As a result, the chosen modeling approach showed promising results in predicting the stiffness of a porous Ti-structure under the application of a compressive stress, which is a crucial property for biomedical applications. It also emphasized the importance of better pore geometry as well as pore dispersion control throughout the fabrication process, as anisotropic features as well as stress concentrations might easily emerge.

In a similar study, Cuadrado et al. [68] investigated the mechanical characteristics of three kinds of porous titanium-alloy structures under compression as well as torsional stresses (normal cubic, body-centered-cubic, as well as cubic made to 45°). The cubic structures were investigated for different load orientations. Human bone has a wide range of mechanical properties based on the kind of bone as well as the weights that are applied. Scaffolds fabricated by electron-beam-melting (EBM) help in achieving and satisfying some of those mechanical properties. The three kinds of porous titanium alloy structures with varied porosities were fabricated in order to evaluate their mechanical properties. The cubic structures were studied using the finite-element approach for various load directions. Abaqus 6.14–2, a Finite-Element program, was used to generate the cubic porous structures. The models were segmented, smoothed, and then reassembled using the Scan IP module. Following that, the models were uploaded immediately into the Scan-FE module, which turned them into volumetric mesh. However, considering the

geometric complexity of the structures, the researchers decided to choose a ten-node tetrahedral-element (C3D10) as the mesh element after completing the requisite sensitivity testing. On the basis of the stress-strain curve obtained from experimental test data, an isotropic plasticity model was developed and was subjected to the FE models. The material properties utilized in the elastic model were given to be 93 GPa for the elastic modulus as well as 0.3 Poisson's ratio, whereas for the plasticity model, 869 MPa yield stress was given. In order to simulate the boundary condition of the compression experiments, the bottom portion of all the cubic structures was set to be fixed, then a load was mounted on the top portion. As expected, cubic structures had higher strength as well as stiffness values when compared to those of body-center-cubic and cross structures when the force was vertically applied. This is due to the fact that the buckling process is dominant in certain structures. This has previously been shown by a number of different authors [69,70]. Also, cross structures, were observed to have superior shear modulus as well as shear strength when compared to cubic structures. The cross structure (cubic structures formed at 45°) and the Body-Center-Cubic under compression had comparable mechanical characteristics, while the former was slightly greater and the latter was substantially lower when compared to the cubic structures. This observation was attributed to the bending mechanism that is dominant in both the cross structure as well as the body-center-cubic structure (Fig. 5). The numerical analysis demonstrated that the cubic structures went directly from buckling into bending deformation as

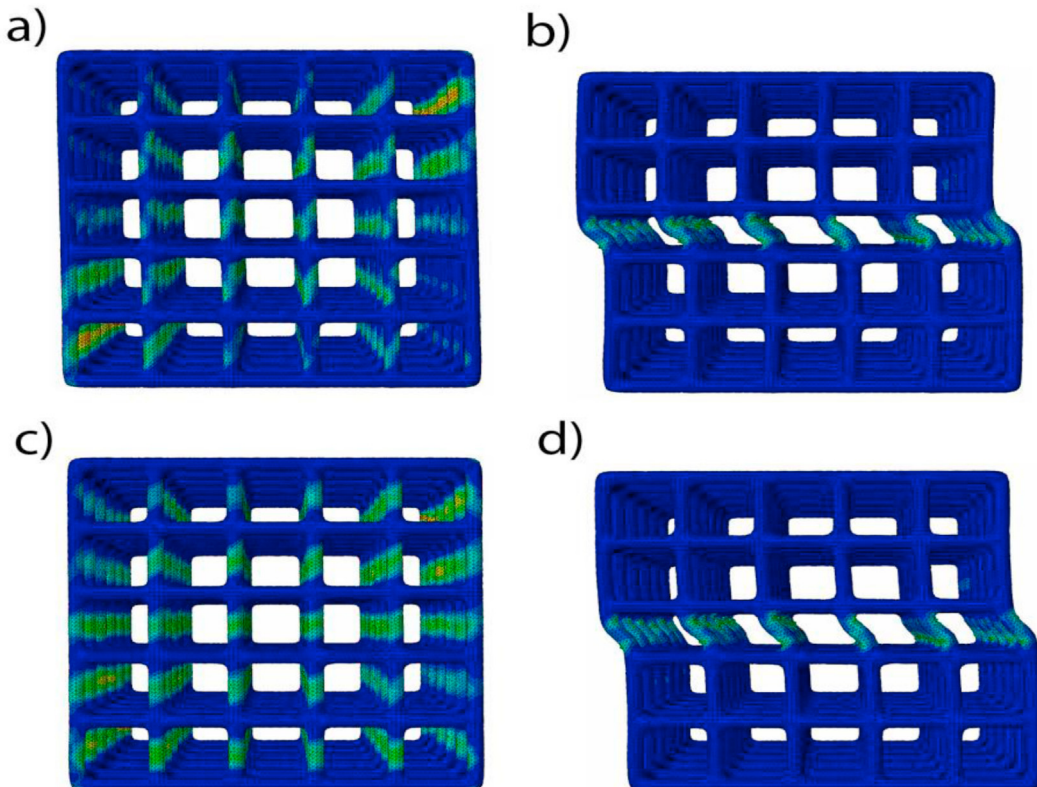


Fig. 5 – Strain and deformation mechanism right before and after the collapse began for loads of 45° , a) and b); and 90° , c) and d); with respect to the horizontal axis (Cuadrado et al. [68], culled with permission from Elsevier).

the orientation angles of the stresses with regard to their horizontal axis were reduced. This resulted in a decline in their mechanical strength. Unlike the BCC and cross structures, which fractured at 45° through band formation, the cubic structures broke down through layer-by-layer collapse. Finally, the authors proposed that all load orientations that an implant or a scaffold is exposed to, as well as other forms of loads that may inevitably arise, such as torque, be taken into consideration while creating and choosing the ideal typology in the rehabilitation of bone defects.

The effect of nano-porous layers fabricated by powder-mix electrical discharge machining on Beta-Titanium was investigated by Prakash et al. [71]. To increase the biocompatibility of beta-phase titanium alloy, the powder mixed electrical discharge machining (PMEDM) approach was utilized to form a nano-porous layer. To increase bio-mechanical anchoring, the PMEDM technology was employed to create a biomimetic new nano-porous layer directly on the Beta-phase Titanium alloy-based implant. The powder mixed electrical discharge machining results in a micro-rough surface layer with a high ratio of interconnected nano-porosities (200–500 nm). An in-vitro bioactivity study was used to assess the vitality as well as the mineralization of the human osteoblast-like cells within a nano-porous surface fabricated by the PMEDM. To determine the tensile as well as the shear strength of the bone-implant contact with various surface topographies (untreated, PMEDMed, and EDMed), a 3-dimensional Finite Element model of the bone/implant interface was created with ANSYS®2014 using APDL code to simulate the bone/implant interface. All models' mechanical behaviours were forecast in terms of deformation and apparent stress in relation to the applied stresses. In order to translate the reaction force against displacement responses of each model to tractions against deformation, the cross-section region of the bone-implant interface was divided. For three load instances (at 0°, 45°, and 90°), Fig. 5 displays the expected apparent stress against deformation. The type of surface porosity and bone ingrowth were discovered to have significant correlations. It was also discovered that surface adhesion to bone tissues increases as the surface nano-porosities increase. This increase in bone/implant interface strength in the EDMed and PMEDMed surfaces is higher than that obtained for the plane surface. The surface nano-porosities on an EDMed and PMEDMed surface generate a greater surface area for bone ingrowth and also provide a better interlocking strength against the applied load. In comparison to EDM and flat surfaces (non-porous), the PMEDMed surface has a larger density of porosities, resulting in a highly strong bone/implant adhesion as well as proliferation of osteoblastic like cells. It was also observed that PMEDM nano-porosity resulted in a 3-fold increase in shear strength and a 4-fold increment in tensile strength. It's also worth noting that the interconnected porosity structures of various sizes had better tensile strength. It was stated that the interface's porosity density is of great importance for bone ingrowth and implant stability in real implants. Future studies are needed to evaluate the interfacial strengths of powder mixed electrical discharge machining prepared nano-porous implants with a more realistic level of porosity. The porous structures investigated here were chosen for their simplicity and ease of research. The impact of a nano-

porous surface on the fatigue strength of the bone/implant interface should also be investigated.

To give guidance for the appropriate design of additively produced porous orthopedic implants and bone replacements, Yu et al. [72] explored three distinct topological porous structures (primitive, BCC, and gyroid) with a porosity level of 65 percent. The structures were designed and produced by selective laser melting. The goal was to provide guidance for the design of additively fabricated porous titanium-based implants for bone replacement applications. Ti–6Al–4V powders were employed for the production of the porous scaffolds. The mechanical strength of the produced scaffolds was evaluated utilizing quasi-static compression and tensile testing. The deformation behavior of the three distinct kinds of porous specimens was carried out using ANSYS 17.0. The following material attributes were included in the model: a modulus of 110 GPa, a Possion's ratio of 0.3, as well as an ultimate compressive strength of 1096 MPa. Finite element simulation was used to examine the deformation behaviors of porous materials under various compression strains and loading conditions. The top surface of unit cells was subjected to compressive and tensile loading forces of 100 N, 200 N, and 300 N, with the bottom surface acting as a permanent support. The compressive and tensile strengths of gyroid scaffolds are 392.1 MPa and 321.3 MPa, respectively, more than twice as much as BCC scaffolds. Fig. 6 depicts the stress distributions within each unit cell. The cross-sectional area of each unit cell with maximum stress perpendicular to the loading direction was measured based on the FE findings. It can be seen that the G-scaffold has the highest cross-sectional area at the maximum stress cross section, which was proposed as the main reason the structure has the best compressive and tensile strength and also transmits stress better in the loading direction than the other types of porous specimen. The cross section of maximum strain and stress at various compressive strains was obtained in order to fully comprehend the crack initiation. The fracture zone corresponded to the center of the unit cells, where the P scaffold's stress concentration regions were located. As with the G scaffold, the stress concentration region was around 45° to the Z axis. For this reason, the G scaffold was more resistant to cracking. The B scaffold's stress concentration is on the struts' connection, and it was found that this place broke first. Similar to the findings reported by Zhang et al. [50], peak compressive strain was found in the thinnest region of the connecting strut of BCC structures. Also, the permeability of the porous specimen was assessed by employing the falling head technique, and the result was compared to the computational fluid dynamics findings. The permeability of the Gyroid scaffolds was found to be around 20 percent higher than that of the BCC scaffolds. It was proposed that the internal design of a porous Ti-based scaffold might have a considerable impact on mechanical stress as well as the permeability of the scaffolds.

2.4. Miscellaneous rehabilitation

The study on hip prosthesis mechanics have been based on static loading assumptions [73,74] but in reality, the hip prosthesis is regularly subjected to dynamic as well as cyclic

Compression

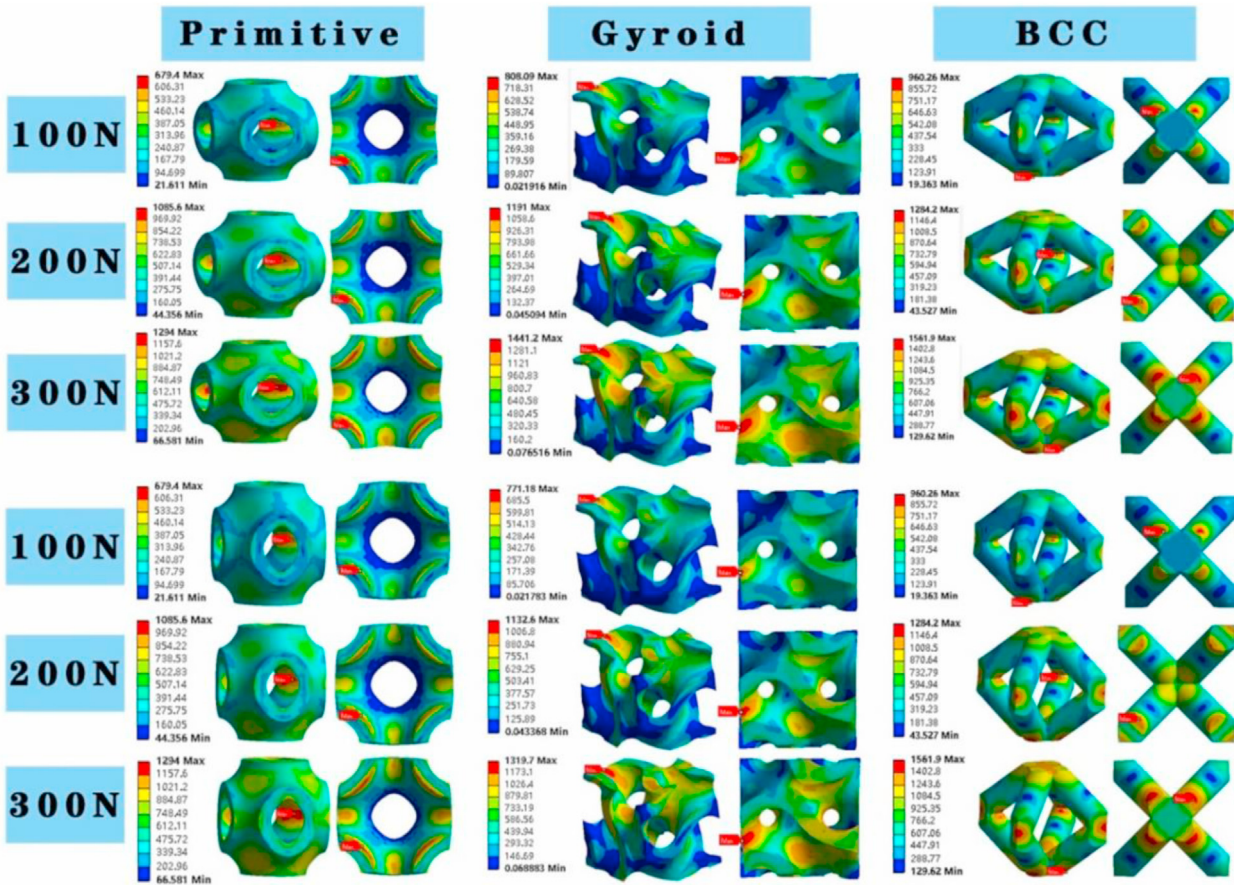


Fig. 6 – FE analysis of the three types of unit cells at loading condition (Yu et al. [72] culed with permission from Elsevier).

stresses during walking, leaping, and climbing. Consequently, understanding the fatigue behaviour of biomaterials intended for hip prosthesis design is very important to avert premature and unexpected implant failure. Aghili et al. [75] conducted a fatigue study on hip prosthesis geometries for different bi-metallic materials in order to predict the most reliable material under fatigue loading. In this study, a 72-year-old patient was selected, and his hip computed tomography scan pictures were utilized to generate the geometry. The authors used four different metallic biomaterials which include: Titanium (Ti), Cobalt-Chrome (Co-Cr), Ti-6Al-4V alloy (Ti-alloy), and Stainless Steel (SS). These prosthesis' material properties were gathered from literature. The developed models were exported into Ansys Workbench for numerical analysis, and for each material, the Von-Mises criterion, deformations, and fatigue life were computed. Geometry reconstruction as well as mesh production were completed successfully, and mesh sensitivity evaluations were validated and confirmed. The maximum Von-Mises stress on the superior line of the stem neck exposed to a static loading scenario was examined, and the lowest values (that is, 591 MPa) were recorded in Ti prosthesis compared to other metallic biomaterials. When a pure Ti stem was compared with Ti-alloy, SS, and Co-Cr stems, the maximum sustained von-Mises stress rose by 4.91 percent, 8.80 percent, and 9.64 percent, respectively. The stress distribution followed the same

patterns during cyclic loading, with the highest stress on the superior line of the stem neck measured at 687 MPa, 721 MPa, 748 MPa, and 753 MPa for titanium, titanium alloy, stainless steel, and cobalt-chrome, respectively. The maximum safety factor (that is, 1.54) was reported for pure Ti, which dropped 11.03 percent, 18.83 percent, and 20.12 percent when compared to the Ti-alloy stem, stainless steel stem, and cobalt-chrome stem, respectively. The overall deformation of the materials under cyclic loading was investigated. Computed deformations for all of the aforementioned materials showed no significant difference. The authors established that pure titanium is the most appropriate material for hip prostheses owing to its lower stress concentration as well as longer life span when compared to other metallic biomaterials examined in this study. These results are in agreement with the findings reported by Mughal et al. [76] and Tang et al. [77]. A typical strategy for verifying numerical simulations is to leverage on existing *in vivo/in vitro* data. The authors, however, simply compared the derived numerical findings to previously published data. As a consequence, more research should be conducted to collect experimental data in order to verify and provide credible interpretation of the findings from the study.

Using finite element analysis, the biomechanical effects of implant diameter for dental application, type of connection, as well as bone density on micro-gap generation and fatigue

failure were studied by Lee et al. [78]. This study looked into the micro-gap creation and fatigue failure in orthodontic implants, screws, and abutments based on bone density, implant diameter, and connection type, in a variety of clinical contexts. Twelve 3-D finite element models were generated by integrating three implant diameters (3.5 mm, 4.0 mm, 4.5 mm), two connection types, as well as two bone densities (high and low). Each model includes the implant system, nerve canal, as well as cortical and cancellous bone tissues. After the screws were preloaded, oblique (200 N) and vertical (100 N) loadings were applied. The researchers evaluated the comparative displacements across the implant, abutment, as well as the screw's interfaces. The fatigue lives of Ti–6Al–4V alloy components were calculated using repetitive mastication models. Mann–Whitney U as well as Kruskal–Wallis one-way assessments were conducted on each model's top Fifty displacement values. Substantial micro-gaps just at the implant/abutment interface were found under oblique stress in the buccal axis. At the abutment/screw interface, micro-gap creation rose around the implant diameter during vertical loading but declined under oblique loading condition; the lingual direction exhibited the most micro-gap formation. In all cases, the bone-level connection created more micro-gaps when compared to the tissue-level connection. To better reflect real-world oral circumstances, one cyclic loading consisted of one vertical as well as one oblique loading was employed in the fatigue failure simulation. In this investigation, one million loading cycles corresponded to approximately ten years of survival was utilized. All of the implant-tissue models withstood up to 107 vertical as well as oblique loading cycles, indicating that the tissue-level implants are much more resistant to fatigue failure throughout their entire life. The abutment of the implant-bone models with implant sizes of 4.0 and 4.5 mm lasted 500,000–1,000,000 loading cycles prior to fatigue failure, equating to 5–10 years. Only those bone-level connection models with a benchmark fatigue life of 3.5 mm for the implant diameter indicated fatigue failure within 1000 loading cycles; this might indicate that the abutment connection area's wall thickness was insufficient to survive the cyclic stress on the molar area (Fig. 7). The statistics indicate that the type of connection and implant diameter are major drivers of implant system biomechanical behavior. As opposed to bone-level implants, tissue-level implants have biomechanical advantages. In the posterior mandibular area, two-piece implants with a diameter of less than 3.5 mm should be avoided.

Cervical spondylosis is a prevalent condition characterized by degeneration of the cervical spine that affects more than half of the world's elderly population. As the disease's prevalence continues to rise, it has become a worldwide subject of concern [79,80]. Due to a scarcity of research concentrating on titanium mesh cage size, surgeons are concerned as to how to establish the appropriate size of cage to offer surgical segments with suitable distraction. Zhou et al. [81] used the finite element approach to investigate the biomechanical reactions of the cervical spine following the implantation of cages of varying heights and trimming angles. Twenty Anterior Cervical Corpectomy as well as Fusion models were created, with the surgical section being C5. These models corresponded to combinations of four varying heights and five different

trimmed angle cages. The biomechanical variables were estimated using simulated physiological stress of the cervical spine. A rating system was developed to completely examine the biomechanical capabilities of titanium mesh cages with varying heights and trimmed angles, aiding in the selection of the most optimal combination of cage height as well as trimmed angle. It was suggested that in the single-level anterior cervical corpectomy and fusion at the C5 segment, a titanium cage with a height fitting the space between C4 and C6, as well as a trimmed angle 2° lower than the sagittal angle of the C4 inferior end plate, would provide the cervical spine with an appropriate biomechanical environment to prevent cage collapse and lessen the effect on nearby portions of the spinal column. It was concluded that the height of the titanium mesh cage and the angles at which it is trimmed have a considerable impact on the biomechanical reactions of the cervical spine. When the FE model output was compared to in-vitro experimental data gathered from literature, the FE model produced in this work predicted cervical movements in close agreement with the experimental data and was therefore declared verified. The findings of this research would provide quantitative direction for surgeons in determining the appropriate height and trimming angle of a titanium mesh cage for a particular patient in order to obtain positive clinical outcomes. This research does have some drawbacks. The support of the muscles, which is vital in cervical motion, was not taken into account. Furthermore, material qualities, contact relationships, and loadings were simplified, making it impossible to accurately replicate the true *in vivo* biomechanical and biological environment.

Using the finite element method, Lee et al. [82] studied the biomechanical reaction of lumbar spine segments and porous cages right after the surgery and following bone fusion, as well as the different posterior lumbar interbody fusion (PLIF) procedures' long-term effects. By employing three PLIF procedures, the biomechanical responses of titanium cages (50% porosity and 1 mm pore diameter) as well as the lumbar segments integrated with these cages were assessed (a single cage at the inter-vertebral space's center, a single cage half-anteromedial to the inter-vertebral space, and two cages bilateral to the inter-vertebral space) with bone ingrowth and without bone ingrowth. The stability of the lumbar segments with porous cages without any posterior instrumentation was improved by the fusion of the bone, and the peak of the von Mises stress decreased in the porous cages and the cortical bones, according to the findings. Under both bone fusion circumstances, the bilateral placement of two cages in the intervertebral space is said to have attained the maximum stability of the structure in the lumbar segment and the lowest von Mises stress in the cage. When compared to no-fusion models, the single cage range of motion reduced by 11 percent (from 1.18 to 1.05°) in the intervertebral space center during flexion and by 66.5 percent (from 4.46 to 1.5°) under identical loading during extension (2-Nm). With PLIF, two porous titanium cages, each with a porosity of 50%, can provide good lumbar segment stability. If just one cage is available, it is recommended that the cage be placed in the intervertebral space half-anterior to manage deteriorated lumbar segments. There were some limitations to this investigation. First, medical photographs of a healthy patient with

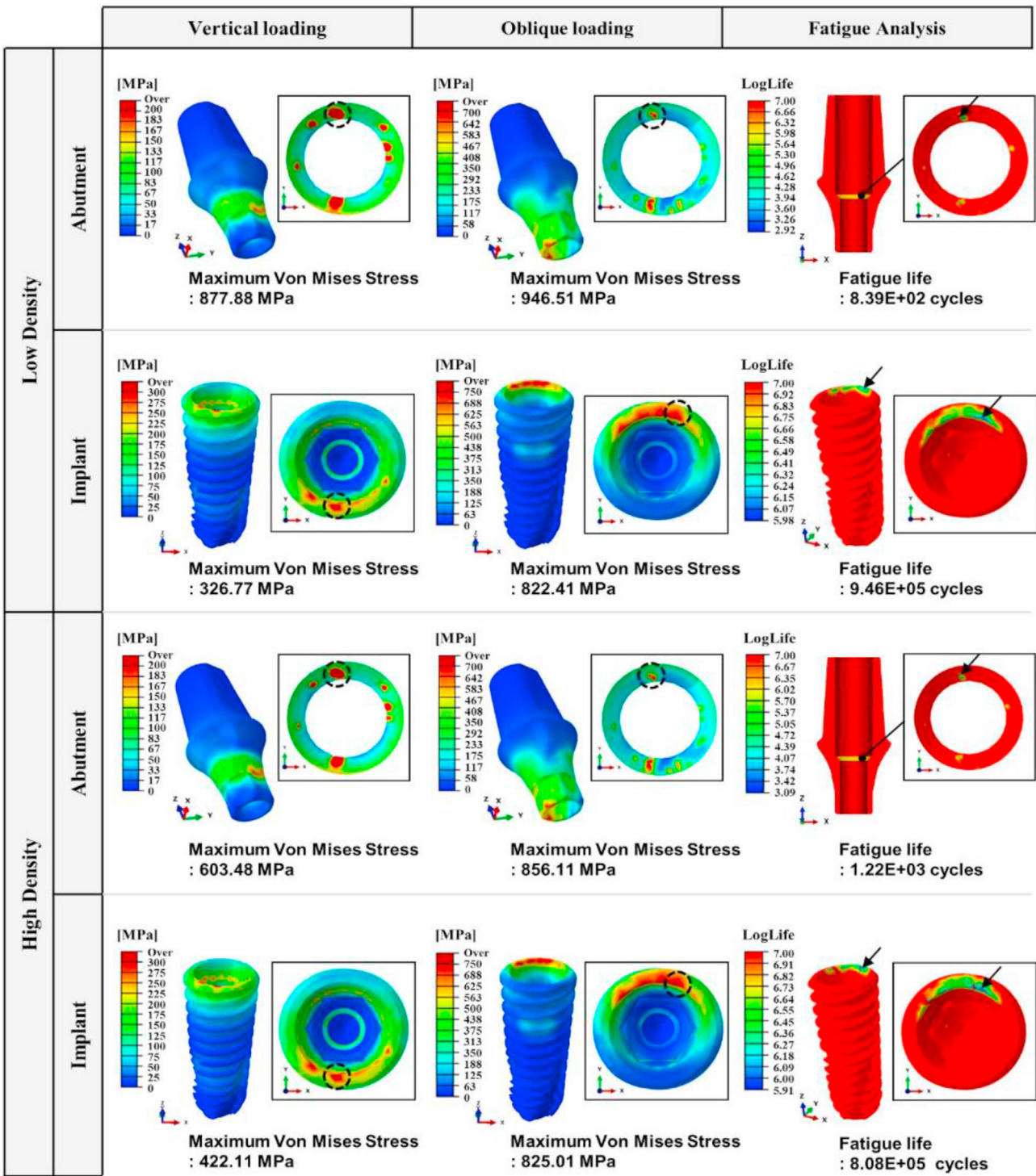


Fig. 7 – Von Mises stress distribution and fatigue analysis results for the internal bone connection case, implant diameter of 3.5 mm, and low density bone. The yellow regions for abutment and arrows indicate the areas of predicted fractures (Lee et al. [78], culed with permission from Elsevier).

no spine pathology were used to create the model. L3-L4 segment was kept in its natural (neutral) position in this investigation because during the PLIF simulation, stable vertebral body coordinates were maintained. The deteriorated disk collapses in clinical practice, and the disk space is

restored based on their experience. Secondly, cages used had a porosity of 50% (in addition to full bone ingrowth). Cages with varying porosities and partial bone ingrowth were not investigated. To make simulations easier, it was assumed that all the materials were homogeneous and also isotropic.

Nevertheless, this assumption may be incorrect for multi-directional loading circumstances. Because the other lumbar segments would have necessitated enormous calculations for the number nodes and components, only one motion segment was addressed in this simulation. The conclusion of the study is completely based on the current FE model. However, results may differ when additional motion segments are developed and examined. Finally, the trunk muscles were ignored, which could lead to a loss of stability if the muscular contraction forces are insufficient. Early loading of titanium dental implants with a rough surface placed without the use of modern surgical techniques has become standard practice. Aside from advancements in loading techniques, the strength of traditional implants made from titanium implant material has recently been improved by converting them into a unique titanium–zirconium (TiZr) alloy, which was originally designed for the improvement of the fatigue performance of narrow-diameter implants. The goal of this method is to have narrow-diameter titanium implants with mechanical qualities comparable to those of standard-diameter titanium implants when it comes to crucial treatment planning. It is believed that less advanced surgical procedures will be used to reduce healing time and the danger of biological problems.

Maxillofacial plates and implantable devices made of titanium alloy are commonly employed in fracture therapy and reconstruction. Jindal et al. [83] used FEM to investigate the effect of Graphene Nanoplatelets (GNPs) filler material, as well as the plate design configurations, on the mechanical characteristics of maxillofacial plates made of Titanium alloy. FE Model was created to recreate a shattered human mandible, and a pure Titanium Alloy based plate model was fine meshed (8924 mesh elements for the plate, 1598 for the screws, and 52526 for the mandible). A compression static simulation investigation was performed on the mandible with defined (50N and 500N) biting forces. Both biting forces (50N and 500N) were applied to the mandible, and the stress distribution throughout the plate segments was evaluated using Von-Mises failure theory. A pure plate was severely strained at a portion at the mandibular fracture site with a Von-Mises stress of almost 27.5 GPa, however this stress was minimized by roughly 10–22% with the inclusion of small GNPs in the plate. GNPs oriented parallel to the plate axis (21.1 GPa) were more effective than other orientations (90, 45, and 135), and location adjustment of these Graphene Nanoplatelets along the plate had no significant influence on the stress distribution. The fatigue studies revealed that, at these loads and strains, the plate containing GNP could last over 7000 days, whereas the pure Titanium alloy plate might fail through fatigue in around 70 days. As a result, the inclusion of small compositions of GNPs may improve Titanium plate endurance life by lowering stress concentrations at crucial parts of the plate. The parallel orientation of GNPs produced better results, which might be attributed to the geometrical layout of the applied stresses and fracture site. According to the author, GNPs in parallel direction worked as fixed beam reinforcement between the mandibles, minimizing stress distributions in the plate and absorbing a large portion of the stress along their own layers. Because GNPs have a greater elastic modulus and tensile strength than Titanium alloy, lesser stresses are imparted to the plate, enhancing its

resistance to failure. Li et al. [84] reported similar findings. However further research should be conducted using the same geometrical layout by altering the depth, weight, and size of GNPs.

3. Challenges and future directions

The implementation of computational approaches keeps advancing across different fields over the years. The utilization of finite element analysis, among other computational approaches, as a substitute for real experiments and aimed at overall cost effectiveness is greatly improving. In biomedical applications, among other fields, it has proven to be reliable for the design of prostheses, the development of osteosynthesis, as well as the quality optimization of implants. Currently, a lot of finite element analysis of biomaterials has been carried out with some of the existing software. However, some shortcomings have been noted regarding their use in analyzing biomechanical competencies of titanium-based biomaterials (extendable to other biomaterials). The challenges are primarily (1) the difficulty of simulating accurately the dynamic activities of the specimen (organs) [85], and (2) the challenge of simulating (or validating with) in-vivo processes [4].

The challenge of simulating the dynamic activities of biomaterials has been an age-long problem. This can be attributed to a lot of factors and assumptions, such as time for data collection and monitoring, which are used during FE analysis. The short time often used for data collection and monitoring may not truly represent the lifetime period the biomaterial is expected to be in use. Similarly, limited data for analysis (due to a factor such as unavailability of patients), could affect the prediction and reliability of the outputs from FEA assessments, as the research development over time depends on existing data. In addition, considering the high stiffness of titanium and its alloys, it is difficult to simulate accurately the biomechanical behaviour of titanium implants for different age ranges (for instance, infants and adults) as the same property input is usually used for the simulation [8,9,29]. The existing assumptions that are mostly utilized for FEA analysis include: concentrated/point loading conditions, material properties in a known media or environment similar to where it is located, a particular activity (or movement) and a known range (and direction) of loading the specimen (organs), among other assumptions [29,41,45]. However, most of the bioactivities and bioprocesses are dynamic, for instance, the effect of bone remodeling on the implant. In addition, implants are developed on a general basis (e.g., age or gender) but the effect in a growing human with dynamic changes over time are not usually considered [29,37]. There are also problems due to the loading strategy where concentrated forces are considered, whereas most of the bone activities are dynamic (relating to fatigue and continuous deformation) and this results in a negligible difference between the predicted and the real properties of biomaterials and implants [4,8]. Another factor is the orientation of the loading, as axial loads are usually considered, but there could be the influence of other forces from other organs/parts in contact (e.g., at a joint) [8,46]. Hence, there is a need for research to move beyond working

with the classical assumptions and to work with new statistics to develop algorithms that are peculiar to a certain group (in terms of age group), and scenarios (in terms of loading orientation and property assumptions). For instance, algorithms considering distributed/changing loads would be a starting point for the prevailing complexity of fatigue analysis with the use of FEA [29,37].

The proposed future directions to solve the dynamic problem are connected with the second challenge of validating biomaterials with in-vivo processes. This challenge can be solved on one hand with the collection and monitoring of patients and the development of advanced equipment or the improvement of existing equipment. Thus, collection of data over the lifetime of the implant, advanced equipment, coupled with the willingness of the patients, is important in solving this.

Thus, a synergy of physical and computational bio-models and cooperation between researchers and patients would help to solve the existing challenges and, more importantly, enhance the selection of accurate mathematical models for biomechanics problems [33,45,85]. Moreover, the use of human organs instead of those of animals (rabbit, mouse, pig) would be more beneficial in predicting biomaterials and their functions. In addition is the intense research needed to develop approaches that could simulate the dynamic multi-part specimens and multi-processes similar to the body instead of considering discrete biological processes. In other words, future research into new concepts of analyzing the effects of cyclic (dynamic) loading over a long time, accounting for the different movements of the part and its varying activities are difficult to model, and development (of new) or full exploitation of existing equipment and software should be fortified.

4. Conclusion

This article provided an in-depth overview of the applicability of finite element analysis in optimizing selection and design of titanium-based biomaterial systems proposed for fractures and tissues rehabilitation. Appraising the use of FEA method in fracture repairs such as femoral, mandible, orthodontic, maxillofacial, hip prosthesis, among other tissue rehabilitation interventions, attested to the high promise of FEA based computational modeling and simulation approach for evaluating material behaviour and optimizing Ti-biometallic systems design. The studies reviewed highlighted the significance of materials, design, and modeling parameters, as well as validation routines on the accuracy and practicality of simulation results and outcomes. Despite some observed challenges, the generated computational data were observed to agree significantly with trends from experimental studies, and exhibit enormous potential for practical applications.

Author Biography

Kenneth Kanayo Alaneme – is Professor of Metallurgical and Materials Engineering at the Federal University of Technology, Akure, Nigeria; and currently Visiting Professor with the

University of Johannesburg, South Africa. He currently has close to 200 well cited articles published in high impact Journals and peer reviewed conference proceedings.

Sodiq Abiodun Kareem – is a Master of Engineering Graduate Student in the Department of Metallurgical and Materials Engineering, Federal University of Technology, Akure, Nigeria.

Blessing Ngozi Ozah – is a PhD candidate in the Department of Metallurgical and Materials Engineering, Federal University of Technology, Akure, Nigeria.

Hassan A. Alshahrani – is currently Assistant Professor and Chairman of Department of Mechanical Engineering, Najran University, Najran, Saudi Arabia. He has several articles published in High Impact SCI indexed Journal and Conference Proceedings.

Oluwadamilola Abigael Ajibawa – is a Master of Science Graduate Student in the Institute for Materials Science, Faculty of Engineering, University of Kiel, Germany.

Declaration of Competing Interest

The authors declare that they have no known competing financial interests or personal relationships that could have appeared to influence the work reported in this paper.

Acknowledgement

The authors wish to acknowledge the support received from their institutions; and the lead author acknowledges the support of the National Research Foundation (NRF), South Africa, through Grant No: 138062.

REFERENCES

- [1] Ratner BD, Hoffman AS, Schoen FJ, Lemons JE, Wagner WR, Sakiyama-Elbert SE, et al. Introduction to biomaterials science. *Biomater Sci* 2020;3–19. <https://doi.org/10.1016/b978-0-12-816137-1.00001-5>.
- [2] Agarwal KM, Singh P, Mohan U, Mandal S, Bhatia D. Comprehensive study related to advancement in biomaterials for medical applications. *Sens Int* 2020;100055. <https://doi.org/10.1016/j.sintl.2020.100055>.
- [3] Chakraborty A, Datta P, Majumder S, Mondal SC, Roychowdhury A. Finite element and experimental analysis to select patient's bone condition specific porous dental implant, fabricated using additive manufacturing. *Comput Biol Med* 2020;103839. <https://doi.org/10.1016/j.combiomed.2020.103839>.
- [4] Merema BJ, Kraima J, Glas HH, Spijkervet FKL, Witjes MJH. Patient-specific finite element models of the human mandible; lack of consensus on current setups. *Oral Dis* 2020. <https://doi.org/10.1111/odi.13381>.
- [5] Boccalatte LA, Nassif MG, Figari MF, Gómez NL, Argibay MC, Mancino AV, et al. Computer-assisted surgery for replacement of the temporomandibular joint with customized prostheses: can we validate the results? *Oral Maxillofac Surg* 2020. <https://doi.org/10.1007/s10006-020-00858-3>.

- [6] Abitha H, Kavitha V, Gomathi B, Ramachandran B. A recent investigation on shape memory alloys and polymers based materials on bio artificial implants-hip and knee joint. *Mater Today Proc* 2020. <https://doi.org/10.1016/j.matpr.2020.07.711>.
- [7] Nikkhoo M, Hassani K, Tavakoli Golpaygani A, Karimi A. Biomechanical role of posterior cruciate ligament in total knee arthroplasty: a finite element analysis. *Comput Methods Progr Biomed* 2020;183:105109. <https://doi.org/10.1016/j.cmpb.2019.105109>.
- [8] Crump EK, Quacinella M, Deafenbaugh BK. Does screw location affect the risk of subtrochanteric femur fracture after femoral neck fixation? A biomechanical study. *Clin Orthop Relat Res* 2020;478(4):770–6. <https://doi.org/10.1097/CORR.0000000000000945>.
- [9] Ju FX, Hou RX, Xiong J, Shi HF, Chen YX, Wang JF. Outcomes of femoral neck fractures treated with cannulated internal fixation in elderly patients: a long-term follow-up study. *Orthop Surg* 2020;12(3):809–18. <https://doi.org/10.1111/os.12683>.
- [10] Zaokari Y, Persaud A, Ibrahim A. Biomaterials for adhesion in orthopedic applications: a review. *Eng Regen* 2020;1:51–63. <https://doi.org/10.1016/j.engreg.2020.07.002>.
- [11] Surmeneva MA, Koptyug A, Khrapov D, Ivanov YF, Mishurova T, Evsevlev S, et al. In situ synthesis of a binary Ti6Al4V-Nb alloy by electron beam melting using a mixture of elemental niobium and titanium powders. *J Mater Process Technol* 2020;282:116646. <https://doi.org/10.1016/j.jmatprotec.2020.116646>.
- [12] Prochor P, Frossard L, Sajewicz E. Effect of the material's stiffness on stressshielding in osseointegrated implants for bone-anchored prostheses: a numerical analysis and initial benchmark data. *Acta Bioeng Biomech* 2020;22. <https://doi.org/10.37190/abb-01543-2020-02>.
- [13] Shahin M, Munir K, Wen C, Li Y. Magnesium matrix nanocomposites for orthopedic applications: a review from mechanical, corrosion, and biological perspectives. *Acta Biomater* 2019. <https://doi.org/10.1016/j.actbio.2019.06.007>.
- [14] Liu L, Wang S, Liu J, Deng F, Li Z, Hao Y. Architectural design of Ti6Al4V scaffold controls the osteogenic volume and application area of the scaffold. *J Mater Res Technol* 2020;9:15849–61. <https://doi.org/10.1016/j.jmrt.2020.11.061>.
- [15] Nagentrau M, Tobi ALM, Jamian S, Otsuka Y. HA-coated hip prosthesis contact pressure prediction using FEM analysis. *Mater Sci Forum* 2020;991:53–61. <https://doi.org/10.4028/www.scientific.net/MSF.991.53>.
- [16] Correa DRN, Rocha LA, Donato TAG, Sousa KSJ, Grandini CR, Afonso CRM, et al. On the mechanical biocompatibility of Ti-15Zr-based alloys for potential use as load-bearing implants. *J Mater Res Technol* 2019. <https://doi.org/10.1016/j.jmrt.2019.11.051>.
- [17] Chang Tu C, Tsai PI, Chen SY, Kuo MYP, Sun JS, Chang JZC. 3D laser-printed porous Ti6Al4V dental implants for compromised bone support. *J Formos Med Assoc* 2020;119:420–9. <https://doi.org/10.1016/j.jfma.2019.07.023>.
- [18] Li J, Jansen JA, Walboomers XF, van den Beucken JJ. Mechanical aspects of dental implants and osseointegration: a narrative review. *J Mech Behav Biomed Mater* 2020;103:103574. <https://doi.org/10.1016/j.jmbbm.2019.103574>.
- [19] Almansoori AA, Choung H-W, Kim B, Park J-Y, Kim S-M, Lee J-H. Fracture of standard titanium mandibular reconstruction plates and preliminary study of three-dimensional printed reconstruction plates. *J Cranio-Maxillo-Fac Surg* 2020;78:153–66. <https://doi.org/10.1016/j.joms.2019.07.016>.
- [20] Pei X, Wu L, Lei H, Zhou C, Fan H, Li Z, et al. Fabrication of customized Ti6Al4V heterogeneous scaffolds with selective laser melting: optimization of the architecture for orthopedic implant applications. *Acta Biomater* 2021;126:485–95. <https://doi.org/10.1016/j.actbio.2021.03.040>.
- [21] Cai D, Zhao X, Yang L, Wang R, Qin G, Chen D-f, et al. A novel biomedical titanium alloy with high antibacterial property and low elastic modulus. *J Mater Sci Technol* 2021;81:13–25. <https://doi.org/10.1016/j.jmst.2021.01.015>.
- [22] Lee B-S, Lee H-J, Lee K-S, Kim HG, Kim G-H, Lee C-W. Enhanced osseointegration of Ti6Al4V ELI screws built-up by electron beam additive manufacturing: an experimental study in rabbits. *Appl Surf Sci* 2020;508:145160. <https://doi.org/10.1016/j.apsusc.2019.145160>.
- [23] Chen Z, Yan X, Yin S, Liu L, Liu X, Zhao G, et al. Influence of the pore size and porosity of selective laser melted Ti6Al4V ELI porous scaffold on cell proliferation, osteogenesis and bone ingrowth. *Mater Sci Eng C* 2020;106:110289. <https://doi.org/10.1016/j.msec.2019.110289>.
- [24] Xiong YZ, Gao RN, Zhang H, Dong LL, Li JT, Li X. Rationally designed functionally graded porous Ti6Al4V scaffolds with high strength and toughness built via selective laser melting for load-bearing orthopedic applications. *J Mech Behav Biomed Mater* 2020;104:103673. <https://doi.org/10.1016/j.jmbbm.2020.103673>.
- [25] Falkowska A, Seweryn A, Skrodzki M. Strength properties of a porous titanium alloy Ti6Al4V with diamond structure obtained by laser power bed fusion (LPBF). *Materials* 2020;13:5138. <https://doi.org/10.3390/ma13225138>.
- [26] Liu YJ, Ren DC, Li SJ, Wang H, Zhang LC, Sercombe TB. Enhanced fatigue characteristics of a topology-optimized porous titanium structure produced by selective laser melting. *Addit Manuf* 2020;32. <https://doi.org/10.1016/j.addma.2020.101060>.
- [27] Lascano S, Chávez-Vásconez R, Muñoz-Rojas D, Aristizabal J, Arce B, Parra C, et al. Graphene-coated Ti-Nb-Ta-Mn foams: a promising approach towards a suitable biomaterial for bone replacement. *Surf Coating Technol* 2020;126250. <https://doi.org/10.1016/j.surfcoat.2020.126250>.
- [28] Liverani E, Rogati G, Pagani S, Brogini S, Fortunato A, Caravaggi P. Mechanical interaction between additive-manufactured metal lattice structures and bone in compression: implications for stress shielding of orthopaedic implants. *J Mech Behav Biomed Mater* 2021;121:104608. <https://doi.org/10.1016/j.jmbbm.2021.104608>.
- [29] Umale S, Yoganandan N, Kurpad SN. Development and validation of osteoligamentous lumbar spine under complex loading conditions: a step towards patient-specific modeling. *J Mech Behav Biomed Mater* 2020;110:103898. <https://doi.org/10.1016/j.jmbbm.2020.103898>.
- [30] Glatt V, Evans CH, Tetsworth K. A concert between biology and biomechanics: the influence of the mechanical environment on bone healing. *Front Physiol* 2017;7. <https://doi.org/10.3389/fphys.2016.00678>.
- [31] Rappel H, Beex LAA, Hale JS, Noels L, Bordas SPA. A tutorial on Bayesian inference to identify material parameters in solid mechanics. *Arch Comput Methods Eng* 2020;27(2):361–85. <https://doi.org/10.1007/s11831-018-09311-x>.
- [32] Suzuki T, Matsuura Y, Yamazaki T, Akasaka T, Ozone E, Matsuyama Y, et al. Biomechanics of callus in the bone healing process, determined by specimen-specific finite element analysis. *Bone* 2020;132:115212. <https://doi.org/10.1016/j.bone.2019.115212>.
- [33] Duprez M, Bordas SPA, Bucki M, Bui HP, Chouly F, Lleras V, et al. Quantifying discretization errors for soft tissue simulation in computer assisted surgery: a preliminary study. *Appl Math Model* 2020;77:709–23. <https://doi.org/10.1016/j.apm.2019.07.055>.

- [34] Soufivand AA, Abolfathi N, Hashemi SA, Lee SJ. Prediction of mechanical behavior of 3D bioprinted tissue-engineered scaffolds using finite element method (FEM) analysis. *Addit Manuf* 2020;101181. <https://doi.org/10.1016/j.addma.2020.101181>.
- [35] Yao Y, Mo Z, Wu G, Guo J, Li J, Wang L, et al. A personalized 3D-printed plate for tibialocalcaneal arthrodesis: design, fabrication, biomechanical evaluation and postoperative assessment. *Comput Biol Med* 2021;133:104368. <https://doi.org/10.1016/j.compbimed.2021.104368>.
- [36] Zhong S, Shi Q, Sun Y, Yang S, Van Dessel J, Gu Y, et al. Biomechanical comparison of locking and non-locking patient-specific mandibular reconstruction plate using finite element analysis. *J Mech Behav Biomed Mater* 2021;124. <https://doi.org/10.1016/j.jmbbm.2021.104849>. 104849.
- [37] Choi AH. Stress induced at the bone-particle-reinforced nanocomposite interface. *Interfaces Part Fibre Reinforced Compos* 2020;515–28. <https://doi.org/10.1016/b978-0-08-102665-6.00019-4>.
- [38] Wang G, Tang Y, Wu X, Yang H. Finite element analysis of a new plate for Pauwels type III femoral neck fractures. *J Int Med Res* 2020;48(2). <https://doi.org/10.1177/0300060520903669>. 2020) 300060520903669.
- [39] Lu H, Shen H, Zhou S, Ni W, Jiang D. Biomechanical analysis of the computer-assisted internal fixation of a femoral neck fracture. *Genes Dis* 2020;7(3):448–55. <https://doi.org/10.1016/j.gendis.2019.04.006>. 2020.
- [40] Zhou L, Lin J, Huang A, Gan W, Zhai X, Sun K, et al. Modified cannulated screw fixation in the treatment of Pauwels type III femoral neck fractures: a biomechanical study. *Clin Biomech* 2020;74:103–10. <https://doi.org/10.1016/j.clinbiomech.2020.02.016>.
- [41] Ridzwan MIZ, Sukjamsri C, Pal B, van Arkel RJ, Bell A, Khanna M, et al. Femoral fracture type can be predicted from femoral structure: a finite element study validated by digital volume correlation experiments. *J Orthop Res* 2018;36(3):993–1001. <https://doi.org/10.1002/jor.23669>.
- [42] Zeng W, Liu Y, Hou X. Biomechanical evaluation of internal fixation implants for femoral neck fractures: a comparative finite element analysis. *Comput Methods Progr Biomed* 2020;196:1–8. <https://doi.org/10.1016/jcmpb.2020.105714>.
- [43] Cui Haipo, Wei Wenqing, Shao Yinlin, Du Kewei. Finite element analysis of fixation effect for femoral neck fracture under different fixation configurations. *Comput Methods Biomed Eng* 2021. <https://doi.org/10.1080/10255842.2021.1935899>.
- [44] Mohd Shahjad A, Ganorkar AP. Finite element analysis of femoral intramedullary nailing. *J Res* 2016;2:1–8. ISSN: 2395-7549.
- [45] Demircan Sabit, Uretürk Erdoğan Utku, Apaydın Ayşegül, Şen Sinan. Fixation methods for mandibular advancement and their effects on temporomandibular joint: a finite element analysis study. *BioMed Res Int* 2020;2020:8. <https://doi.org/10.1155/2020/2810763>. Article ID 2810763.
- [46] Gao H, Li X, Wang C, Ji P, Wang C. Mechanobiologically optimization of a 3D titanium-mesh implant for mandibular large defect: a simulated study. *Mater Sci Eng C, Mater Biol Appl* 2019;104:109934. <https://doi.org/10.1016/j.msec.2019.109934>.
- [47] Yamaguchi S, Ancheta RB, Guastaldi FPS, Tovar N, Tawara D, Imazato S, et al. In silico analysis of the biomechanical stability of commercially pure Ti and Ti-15Mo plates for the treatment of mandibular angle fracture. *J Oral Maxillofac Surg* 2017;75(5):1004. <https://doi.org/10.1016/j.joms.2016.12.043>. e1–1004.e9.
- [48] Sandu AV, Baltatu MS, Nabialek M, Savin A, Vizureanu P. Characterization and mechanical properties of new TiMo alloys used for medical applications. *Materials* 2019;12(18):2973. <https://doi.org/10.3390/ma12182973>.
- [49] Niinomi M. Mechanical biocompatibilities of titanium alloys for biomedical applications. *J Mech Behav Biomed Mater* 2008;11:30–42. <https://doi.org/10.1016/j.jmbbm.2007.07.001>.
- [50] Zhang B, Pei X, Zhou C, Fan Y, Jiang Q, Ronca A, et al. The biomimetic design and 3D printing of customized mechanical properties porous Ti6Al4V scaffold for load-bearing bone reconstruction. *Mater Des* 2018;152:30–9. <https://doi.org/10.1016/j.matdes.2018.04.065>.
- [51] Pituru TS, Bucur A, Gudas C, et al. New miniplate for osteosynthesis of mandibular angle fractures designed to improve formation of new bone. *J Cranioma*. 44, 500–505 <https://doi.org/10.1016/j.jcims.2016.01.002>.
- [52] Verestiu L, Spataru M-C, Baltatu MS, Butnaru M, Solcan C, Sandu AV, et al. New Ti–Mo–Si materials for bone prosthesis applications. *J Mech Behav Biomed Mater* 2021;113:104198. <https://doi.org/10.1016/j.jmbbm.2020.104198>.
- [53] Sharma Mehek, Soni Manoj. A musculoskeletal finite element study of a unique and customised jaw joint prosthesis for the asian populace. *Evergreen* 2020;7(3):351–8. <https://doi.org/10.5109/4068615>. 2020–09.
- [54] Shi Q, Sun Y, Yang S, Van Dessel J, Lübbbers H-T, Zhong S, et al. Failure analysis of an in-vivo fractured patient-specific Ti6Al4V mandible reconstruction plate fabricated by selective laser melting. *Eng Fail Anal* 2021a;124:105353. <https://doi.org/10.1016/j.engfailanal.2021.105353>.
- [55] Li C, Liu JF, Fang XY, Guo YB. Efficient predictive model of part distortion and residual stress in selective laser melting. *Addit Manuf* 2017;17:157–68. <https://doi.org/10.1016/j.addma.2017.08.014>.
- [56] Wang J, Liu Y, Rabadia CD, Liang S-X, Sercombe TB, Zhang L-C. Microstructural homogeneity and mechanical behavior of a selective laser melted Ti-35Nb alloy produced from an elemental powder mixture. *J Mater Sci Technol* 2021;61:221–33. <https://doi.org/10.1016/j.jmst.2020.05.052>.
- [57] Palka L, Konstantinovic V, Pruszynski P, Jamroziak K. Analysis using the finite element method of a novel modular system of additively manufactured osteofixation plates for mandibular fractures - a preclinical study. *Biomed Signal Process Control* 2021;65:102342. <https://doi.org/10.1016/j.bspc.2020.102342>.
- [58] Shi Q, Sun Y, Yang S, Van Dessel J, Lübbbers HT, Zhong S, et al. Preclinical study of additive manufactured plates with shortened lengths for complete mandible reconstruction: design, biomechanics simulation, and fixation stability assessment. *Comput Biol Med* Dec 2021b;139:105008. <https://doi.org/10.1016/j.compbimed.2021.105008>.
- [59] Peng W, Cheng K, Liu Y, Nizza M, Baur DA, Jiang X, et al. Biomechanical and Mechanostat analysis of a titanium layered porous implant for mandibular reconstruction: the effect of the topology optimization design. *Mater Sci Eng C* 2021;124:112056. <https://doi.org/10.1016/j.msec.2021.112056>.
- [60] Attar H, Ehtemam-Haghghi S, Kent D, Dargusch MS. Recent developments and opportunities in additive manufacturing of titanium-based matrix composites: a review. *Int J Mach Tool Manufactur* 2018;133:85–102. <https://doi.org/10.1016/j.ijmachtools.2018.06.003>.
- [61] Hrabe N, White R, Lucon E. Effects of internal porosity and crystallographic texture on Charpy absorbed energy of electron beam melting titanium alloy (Ti-6Al-4V). *Mater Sci Eng* 2019;742:269–77. <https://doi.org/10.1016/j.msea.2018.11.005>.
- [62] Attar Hooyar, Ehtemam-Haghghi Shima, Soro Nicolas, Kent, Damon, Dargusch Mathew S. Additive manufacturing of low-cost porous titanium-based composites for biomedical applications: advantages, challenges and opinion for future development. *J Alloys Compd* 2020;827:154263. <https://doi.org/10.1016/j.jallcom.2020.154263>. 154263.

- [63] Bandyopadhyay A, Mitra I, Shivaram A, Dasgupta N, Bose S. Direct comparison of additively manufactured porous titanium and tantalum implants towards in vivo osseointegration. *Addit Manuf* 2019;28:259–66. <https://doi.org/10.1016/j.addma.2019.04.025>.
- [64] Taniguchi N, Fujibayashi S, Takemoto M, Sasaki K, Otsuki B, Nakamura T, et al. Effect of pore size on bone ingrowth into porous titanium implants fabricated by additive manufacturing: an in vivo experiment. *Mater Sci Eng C* 2016;59:690–701. <https://doi.org/10.1016/j.msec.2015.10.069>.
- [65] Han C, Li Y, Wang Q, Wen S, Wei Q, Yan C, et al. Continuous functionally graded porous titanium scaffolds manufactured by selective laser melting for bone implants. *J Mech Behav Biomed Mater* 2018;80:119–27. <https://doi.org/10.1016/j.jmbbm.2018.01.013>.
- [66] Bobbert F, Lietaert K, Eftekhari AA, Pouran B, Ahmadi S, Weinans H, et al. Additively manufactured metallic porous biomaterials based on minimal surfaces: a unique combination of topological, mechanical, and mass transport properties. *Acta Biomater* 2017;53:572–84. <https://doi.org/10.1016/j.actbio.2017.02.024>.
- [67] Soro N, Brassart L, Chen Y, Veidt M, Attar H, Dargusch MS. Finite element analysis of porous commercially pure titanium for biomedical implant application. *Mater Sci Eng, A* 2018;725:43–50. <https://doi.org/10.1016/j.msea.2018.04.009>.
- [68] Cuadrado A, Yáñez A, Martel O, Deviaene S, Monopoli D. Influence of load orientation and of types of loads on the mechanical properties of porous Ti6Al4V biomaterials. *Mater Des* 2017;135:309–18. <https://doi.org/10.1016/j.matdes.2017.09.045>.
- [69] Ahmadi SM, Yavari SA, Wauthle R, Pouran B, Schrooten J, Weinans H, et al. Additively manufactured open-cell porous biomaterials made from six different space-filling unit cells: the mechanical and morphological properties. *Materials* 2015;8(4):1871–96. <https://doi.org/10.3390/ma8041871>.
- [70] Yáñez A, Herrera A, Martel O, Monopoli D, Afonso H. Compressive behaviour of gyroid lattice structures for human cancellous bone implant applications. *Mater Sci Eng C, Mater Biol Appl* 2016;68:445–8. <https://doi.org/10.1016/j.msec.2016.06.016>.
- [71] Prakash C, Kansal HK, Pabla BS, Puri S. On the influence of nanoporous layer fabricated by PMEDM on β -Ti implant: biological and computational evaluation of bone-implant interface. *Mater Today Proc* 2017;4:2298–307. <https://doi.org/10.1016/j.matpr.2017.02.078>.
- [72] Yu Guisheng, Li Zhibin, Li Shuangjian, Zhang Qiang, Hua Youlu, Liu Hui, Zhao Xueyang, Denzel Tafuma Dhaidhai, Li Wei, Wang Xiaojian. The select of internal architecture for porous Ti alloy scaffold: a compromise between mechanical properties and permeability. *Mater Des* 2020;192:108754. <https://doi.org/10.1016/j.matdes.2020.108754>.
- [73] Westerman AP, Moor AR, Stone MH, Stewart TD. Hip stem fatigue: the implications of increasing patient mass. *Proc IME H J Eng Med* 2018;232:520–30. <https://doi.org/10.1177/0954411918767200>.
- [74] Colic K, Sedmak A, Grbovic A, Burzic M, Hloch S, Sedmak S. Numerical simulation of fatigue crack growth in hip implants. *Procedia Eng* 2016;149:229–35. <https://doi.org/10.1016/j.proeng.2016.06.661>.
- [75] Aghili Seyed Arvin, Hassani Kamran, Nikkhoo Mohammad. A finite element study of fatigue load effects on total hip joint prosthesis. *Comput Methods Biomed Eng* 2021. <https://doi.org/10.1080/10255842.2021.1900133>.
- [76] Mughal U, Khawaja H, Moatamed M. Finite element analysis of human femur bone. *Int J Multiphys* 2015;9(2):101–8. <https://doi.org/10.1260/1750-9548.9.2.101>.
- [77] Tang G, Wang J, Luo H. *Sheng Wu yi xue gong cheng xue za zhi*. *J Biomed Eng = Shengwu yixue gongchengxue zazhi* 2015;32(1):73–6.
- [78] Lee H, Jo M, Noh G. Biomechanical effects of dental implant diameter, connection type, and bone density on microgap formation and fatigue failure: a finite element analysis. *Comput Methods Progr Biomed* 2020;1–21. <https://doi.org/10.1016/j.cmpb.2020.105863>.
- [79] Wen Z, Lu T, Wang Y, Liang H, Gao Z. Anterior cervical corpectomy and fusion and anterior cervical discectomy and fusion using titanium mesh cages for treatment of degenerative cervical pathologies: a literature review. *Med Sci Mon Int Med J Exp Clin Res* 2018;246398–404. <https://doi.org/10.12659/MSM.910269>.
- [80] Hu B, Wang L, Song Y, Hu Y, Lyu Q, Liu L, et al. A comparison of long-term outcomes of nanohydroxyapatite/polyamide-66 cage and titanium mesh cage in anterior cervical corpectomy and fusion: a clinical follow-up study of least 8 years. *Clin Neurol Neurosurg* 2019;17625–9. <https://doi.org/10.1016/j.clineuro.2018.11.015>.
- [81] Zhou Enze, Huang Huiwen, Zhao Yanbin, Wang Lizhen, Fan Yubo. The effects of titanium mesh cage size on the biomechanical responses of cervical spine after anterior cervical corpectomy and fusion: a finite element study. *Clin BioMech* 2022;91:105547. <https://doi.org/10.1016/j.clinbiomech.2021.105547>.
- [82] Lee Y-H, Chung C-J, Wang C-W, Peng Y-T, Chang C-H, Chen C-H, et al. Computational comparison of three posterior lumbar interbody fusion techniques by using porous titanium interbody cages with 50% porosity. *Comput Biol Med* 2016;71:35–45. <https://doi.org/10.1016/j.combiomed.2016.01>.
- [83] Prashant Jindal, Frank Worcester, Walia Kartikeya, Gupta Anand, Breedon Philip. Finite element analysis of titanium alloy-graphene based mandible plate. *Comput Methods Biomed Eng* 2019. <https://doi.org/10.1080/10255842.2018.1555244>.
- [84] Li Z, Young RJ, Wilson NR, Kinloch IA, Valles C, Li Z. Effect of the orientation of graphene-based nanoplates upon the Young's modulus of nanocomposites. *Compos Sci Technol* 2016;123:125–33. <https://doi.org/10.1016/j.compscitech.2015.12.005>.
- [85] Dierckx H, Fenton FH, Filippi S, Pumir A, Sridhar S. Editorial: simulating normal and arrhythmic dynamics: from sub-cellular to tissue and organ level. *Front Phys* 2019;7. <https://doi.org/10.3389/fphy.2019.00089>.